

1 **Supplementary information**

2 **SI.1 Methods**

3 **SI.1.1 Meteorological data compilation**

4 QML(QumaLai), TSH (TianshuiHai), SQH (ShiquanHe), ZD (ZhiDuo), MA (MangAi), GZ (GaiZe),
5 WQ (WenQuan), QSH (QingshuiHe), and ZAD (ZaDuo) can be downloaded from the
6 meteorological data service center, China (<http://data.cma.cn/>), whereas BLH (Beilu'He), KXL
7 (Kaixinling), AD (Anduo), XD(XidaTan), and HSX(HuashiXia) were provided by the State Key
8 Laboratory of Frozen Soil Engineering (SKLFSE), China (<http://sklfse.nieer.ac.cn/>). The approach
9 to address the data gaps is described in ref. 1 and 2. We used linear interpolation to address the
10 dataset gaps if they were less than 2 hours, and we used a method described in ref. 3 to
11 address gaps greater than 2 hours but less than 1 day. Furthermore, we used an artificial neural
12 network approach as described in ref. 4 to fill gaps greater than 1 day.

13 Air temperature was measured by a 2 m tower, and the air temperature sensor was GB10589–
14 89 (Yueke, Chengdu, China). In addition, during 1995–2002, the air sensor was HMP45C
15 (Campbell, Logan, UT 84321–1784, USA), and from 2003 to 2017, the sensor was replaced by
16 HMP155A (Campbell, Logan, UT 84321–1784, USA). From 1975 to 2002, precipitation data were
17 measured by ZGQX–95 (Zhongguoqixiang, Beijing, China), and from 2003 to 2017, precipitation
18 data were measured by T200B (Geonor, Oslo, Norway).

19 Soil temperatures in the 0–50 cm and 50–100 cm soil layers prior to 1990 were measured
20 manually once or twice per month using a mercury thermometer (with an accuracy of ± 0.2 °C).
21 From 1990, all soil temperatures were measured using a string of thermistors made by the
22 SKLFSE (Lanzhou, China). The soil water contents (SWCs) of the 0–50 cm and 50–100 cm soil
23 layers prior to 1995 were calculated gravimetrically using the ratio of the water mass present to
24 the oven–dried (75 °C, 24 hours) weight of the soil sample 1~3 times per year. Since 1995, SWC
25 has been measured by a pF–meter sensor (GEO–Precision, Environmental Industry Companies,
26 Ettlingen, D-76275, Germany).

27 All the above data obtained by the different sensors were calibrated by the Meteorological
28 Data Service Center of the SKLFSE, China.

29 Following Muller's original definition, the maximum active layer thickness (ALT) is the maximum
30 thawing depth in late autumn using a linear interpolation of the temperature of soil profiles
31 between two neighboring points above and below the 0 °C isotherm, as previously described
32 (5).

33 Growing degree day (GDD) is often used to quantify temperature or heat requirements for
34 plant development and is the cumulative sum of air temperatures above a certain degree. GDD
35 is a heuristic tool in phenology that is widely used in mechanism-based phenological models
36 (6). Here, GDD is calculated as the cumulative sum of daily air temperatures above 0 °C
37 following ref. 7.

38 **SI.1.2 Soil property data compilation**

39 All soil cores were taken as two pseudoreplicate cores within 0.5° × 0.5° (latitude and longitude)
40 and from the same vegetation type. The nine locations (AD, QML, BLH, HSX, TSH, SQH, ZD, MA,
41 and GZ) had 62 plots and 1078 cores that were studied in 1975 and 1978 and from 1995 to
42 2017 (26 years). The 5 locations of WQ, QSH, KXL, ZAD and XD had a total of 96 plots and 760
43 cores, which were studied from 2002 to 2017 (16 years).

44 For each soil core, samples from 0–100 cm were collected by a soil corer (diameter is 5 cm) at
45 0–5 cm, 5–10 cm, 10–15 cm, 15–20 cm, 20–30 cm, 30–40 cm, 40–50 cm, 50–100 cm, and for
46 the soil between 100 cm to 500 or 550 cm, we used a motorized drill to collect the samples at
47 50 cm intervals. The samples were collected using a stainless steel ring cutter, with three
48 replicates. The permafrost table was determined by the ice content of the core sampling (5, 8).
49 Near the permafrost table, we collected soil samples every 5 cm in the upper and lower 50 cm
50 ranges. All samples were marked and sealed in a 100 ml steel aluminum box, weighed, frozen at
51 –15 °C, and brought back to the laboratory used for soil property analysis.

52 Soil pH was determined by amperometry (DJS-1C, Leizi, Shanghai, China). Five grams of fresh
53 soil was mixed with CaCl_2 (0.2 M) at a ratio of 1 part soil to 5 parts liquid, and then, the pH of
54 the suspension was measured after 1 hour of shaking for each soil sample of a given year.

55 Soil bulk density was calculated based on total fresh weight, soil water content and total soil
56 volume.

57 Soil organic carbon (SOC) of the air-dried soil samples was analyzed using the wet combustion
58 method, Walkley-Black modified acid dichromate digestion, FeSO_4 titration, and an automatic
59 titrator (9, 10).

60 Total nitrogen (TN) was titrated by the Kjeldahl method (Wu et al., 2016) before 2000, and
61 since 2001, it has been measured by an elementary analyzer (Vario EL Three, Elementar,
62 Germany). All the data transitions between the Kjeldahl method and elemental auto-analysis
63 followed the method described in the lecture of the Chinese ecosystem research network
64 (<http://cern.ac.cn>).

65 The ratio between soil carbon and nitrogen (C:N) was then calculated as the quotient of the
66 SOC and TN concentrations.

67 Chloride (Cl^-) was measured by AgNO_3 titration. Calcium (Ca^{2+}) and magnesium (Mg^{2+}) were
68 measured by EDTA titration. Sodium (Na^+) was measured by a blaze photometer (FP6400,
69 JINGMI, Shanghai, China). For more details of the methods, please see the Chinese ecosystem
70 research network, China (<http://cern.ac.cn>), and for primary results, please see Fig. S13

71 Nitrate (N-NO_3^-) was measured by capacity titration (ELIT 8021, Beijing, China) prior to 2000;
72 since 2001, ion chromatography (T6-New Century Spectrophotometer, PUXI, Beijing, China) has
73 been used. The NO_3^- data obtained by the different methods were calibrated by the SKLFSE,
74 China.

75 Ammonium (N-NH_4^+) was analyzed based on soil samples (2008-2017) with the initial moisture
76 content. The soil samples were extracted by 2 M KCl and then quantified using a flow injection
77 analyzer (Autoanalyzer 3 SEAL, Bran and Luebbe, Norderstedt, Germany), and the limit of

78 detection was $0.003 \text{ N mg L}^{-1}$. The NH_4^+ concentration was subsequently calculated as mg N kg^{-1}
79 dry weight (DW) of soil.

80

81 **SI.1.3 Plant trait data compilation**

82 For each plot, species identification, vegetation height, landscape types, characteristics of
83 surface drainage and erosion status were recorded. Plant coverage was measured in the early
84 or middle of September at 5 plots (1 m × 1 m) placed with a 500 m radius of the borehole
85 position. In 1975 and 1978, it was measured based observations by experts. From 1995 to 2007,
86 using the pin-point method, a 10 cm × 10 cm nylon mesh was laid in a 1 m × 1 m plot to
87 estimate the plant coverage. From 2008 to 2017, a US agricultural multispectral camera was
88 used to measure the plant coverage. The difference in plant coverage between the different
89 methods was successfully validated by linear regression ($r^2 > 0.9$.)

90 Plant height was measured by a 10-point frame sample (wind speed < 0.5 m/s). Forty-five
91 degrees slowly downward from the pin, when the pin first hit the target grass leaf, was
92 recorded and calculated as the individual plant height, with 5 repeats. The average of 50
93 samples (10 points × 5 repeats) was recorded as the plant height. Finally, the mean height for
94 the plot was calculated for any given year.

95 The aboveground biomass in September was quantified in three 20 cm × 20 cm subplots within
96 each plot during September, for a total of 15 subplots per site. At each subplot, aboveground
97 biomass was cut using scissors, packed in paper bags and returned to the laboratory, where all
98 samples were filtered through a 1 mm × 1 mm sieve to remove soil, and plant samples were
99 dried at 75 ± 2 °C for 72 hours to calculate the aboveground biomass.

100 To investigate the root vertical distribution pattern of the plant species in the community, a 1.5
101 m depth pit was dug in five 1.5 m × 1.5 m quadrats to measure the maximum root depth after
102 all of the above work was finished. Since 2008, this approach has been replaced by a special soil
103 sample drill device (diameter is 15 cm) designed by SKLFSE, China.

104 The vertical root distribution was based on visually observed fresh roots from the flow water
105 immersion soil core and consisted of three replicates per plot. A mean value was calculated for
106 the maximum root per plot.

107

108

109 Additional deep soil profile samples were collected in areas with retrogressive thaw slumps
110 near study sites. Non of the actual study sites reveal such features. At these sites, roots were
111 followed to the surface and associated with species-specific living plants. Maximum root
112 lengths which could be linked to individual plants were recorded.

113



114

115

116 The photo shows a retrogressive thaw slump. Thawing permafrost and a collapsed landscape has
117 exposed soil profiles to a depth of about 5 m. The main root zone was within the upper 0.5 m and
118 the active layer depth 2.8 m. Species-specific roots were found at least 2.4 m below the surface
119 (shown with an yellow dashed line) and related to *Kobresia littledalei* C. B. Clarke and
120 *Oxytropis pauciflora* Bunge. The location is 55 km North of ZAD (ZaDuo) and described July
121 13, 2021.

122

123 **SI.1.4 Stable isotope ^{15}N data compilation**

124 To quantify if the ammonium released during permafrost thawing can be taken up by plants,
125 210 plots (including 30 control plots) of 6 sites for both group A (ZD, HSX, and XDT) and group B
126 (BLH, AD, and KXL) were set on 5th to 18th September 2017, which is close to the time of
127 maximum active layer depth and corresponds to the end of the aboveground growing season
128 and onset of plant senescence. N release from the permafrost was mimicked by injecting a
129 trace amount of the stable isotope ^{15}N into the soil at the depth of the thawing permafrost
130 front. At each plot isotopically labeled N, 1 g $^{15}\text{N-NH}_4\text{Cl}$, 99 atom%, was dissolved in 50 g
131 deionized water and wrapped in polyvinyl chloride capsule. To avoid interruption to the ground
132 surface environment, a capsule was launched into the thawing permafrost front by a hollow,
133 narrow slope steel drill (Supplementary Fig. S12), and then, a radar (precise: 0.02 m for 500
134 MHz; MALA ProEx, MALA, Sweden) was used to confirm the location of the capsule and plant
135 sample plot.

136 To assess the time-scale of isotope nitrogen uptake by plants, the dominant plant roots of the
137 0-50 cm soil layer and aboveground mass (including leaves and stems) were collected within
138 33×33 cm quarters immediately above the capsule after treatment for 10~15 days, one year,
139 two years, three years and four years. There were six primary dominant species at 6 sites,
140 including 3 deep-rooted species, which were *Carex moorcroftii* Falc. Ex Boott (*Carex*), *Kobresia*
141 *tibetica* Maxim. (*Kobresia*), and *Oxytropis glacialis* (*Oxytropis*), and 3 shallow-rooted species,
142 which were *Heteropappus bowerii* (Hemsl.) Griens. (*Heteropappus*), *Leontopodium*
143 *nanum* (Hook. f. et Thoms.) Hand.-Ma (*Leontopodium*), and *Saussurea arenaria* Maxim
144 (*Saussurea*). It was not possible to macroscopically separate roots for all plant species, but
145 species could be sorted as deep-rooted and shallow-rooted plant species by hand.

146 The stable isotope ^{15}N is naturally present in very low quantities in plants. By adding a trace
147 amount of ^{15}N , N uptake can be measured by determining the excess ^{15}N content compared to
148 the naturally occurring ^{15}N found in the total N pool. Thus, excess ^{15}N , or ^{15}N enrichment, was

149 calculated as the difference in atom% ¹⁵N between the samples from the treated (isotopically
150 labeled) and untreated (natural abundance) plots:

$$151 \quad \text{atom}\%_{\text{excess}} = \text{atom}\%_{\text{sample}} - \text{atom}\%_{\text{nature abundance}}$$

152 Atom% is calculated as:

$$153 \quad \text{atom}\% = \frac{100 \times (\delta + 1,000)}{\delta + 1,000 + \frac{1,000}{R_{st}}}$$

154 where δ is the $\delta^{15}\text{N}$ for the sample (‰), and R_{st} is the $^{15}\text{N}/^{14}\text{N}$ ratio of the international
155 reference material (0.003676). Samples with naturally abundant $\delta^{15}\text{N}$ were collected from the
156 untreated plots at specific species and harvest times. In this study, potential seasonal changes
157 in the natural abundance of $\delta^{15}\text{N}$ in plants and the significant levels of isotopic enrichment
158 showed that the potential temporal variation in $\delta^{15}\text{N}$ was negligible. Excess ^{15}N is expressed as
159 the concentration of excess ^{15}N per N in plant leaves and roots.

160 **SI.1.5 Data quality control**

161 We conducted a multistep hierarchical data-cleaning method (11) to provide quality control for
162 the compiled data as follows:

163 First, soil property data and plant trait data were checked for improbable values, with the goal
164 of excluding likely errors or measurements with incorrect units but without excluding true
165 extreme values. We manually checked plant trait values and excluded only those that were
166 obviously erroneous based on our expert knowledge of these species.

167 Second, for each case, identifying whether a given observation (x) was likely to be erroneous
168 (that is, ‘error risk’) by calculating the difference between x and the mean (excluding x) of the
169 taxon (species or site) and then dividing by the standard deviation of the taxon were conducted
170 since the standard deviation of a trait value is related to the mean and sample size. We checked
171 individual records against the entire distribution of the observations of trait data and removed
172 any records with an error risk greater than 8 (that is, a value more than 8 standard deviations
173 away from the soil property/plant trait mean value). For individual species across the sites, we
174 estimated a species mean per location and removed observations for which the species (plot-

175 level) mean error risk was greater than 3 (that is, the species mean of that site was more than 3
176 standard deviations away from the species mean across all plots from the location).

177 Finally, we compared individual species records directly to the distribution of the values at the
178 plot level. We excluded values above an error risk of 2.25.

179 After the above procedure was conducted, 124 data points (4.7%) were removed for soil
180 properties, and 316 observations/data points (3.8%) were removed for plant traits.

181 In all cases, we visually checked the excluded values against the distribution of all observations
182 for each species to ensure that our trait and soil property data cleaning protocol was
183 reasonable. Furthermore, we found that 124 excluded data points (4.7%) were removed
184 because soil properties were mainly based on the soil surface pH value (71%) and soil surface
185 NO_3^- data (22%), and 316 data points were removed because plant traits were mainly based on
186 the aboveground biomass of September (86%), which was caused by waste or the activity of
187 small mammals, such as *Ochotona curzoniae*.

188 **SI.1.6 Spatial autocorrection and uncertainty estimates**

189 Because the plots included in this study were not uniformly dispersed over the Tibetan Plateau,
190 we examined the potential of locations, such as locations TM, TGL, KXL and BLH, in relatively
191 concentrated plots to drive the overall patterns. To do this, we first examined spatial
192 autocorrelation in the trends in weather parameters, soil properties and plant traits using
193 Moran's I in the R package ltools (12). Moran's I test results ranged from -1 to 1, where -1
194 indicates a perfectly dispersed variable, 0 indicates a randomly distributed variable, and 1
195 indicates that the data are perfectly autocorrelated. We observed that the results ranged from
196 0.001 to 0.018, which suggests that in this study, some variables were weak but had no
197 significant spatial autocorrelation.

198 We conducted an analysis to compare trends, confidence intervals, and significance of trends
199 over two time periods, 1995–2005 ($n = 154$) and 2006–2017 ($n = 168$), to assess whether
200 different locations during observation years influenced the overall trends in active layer
201 warming, active layer moisture, permafrost thawing, soil properties (0-50 cm, 50-100 cm, and
202 100-permafrost front), and plant traits we observed. For each time period, we used a subset of

203 locations that had data for at least 80% of the years within the defined time period. Following
204 the established methods of ref. 13, we calculated a yearly anomaly in the active layer, soil
205 properties, and plant traits for each location as the difference between each year's observation
206 and the long-term mean. We then averaged these anomalies across all locations and used 1)
207 the probability density function to test for a normal distribution and 2) linear regression to
208 calculate the slope, significance, and confidence intervals of these averaged anomalies.

209 **SI.1.7 Climate, permafrost dataset temporal assimilation and group split**

210 To generate a dataset with consistent time scale (year) resolution within and among climate
211 characteristics, soil properties, and plant traits, we extracted and averaged air temperature,
212 total precipitation, soil temperature, and soil moisture for the growing season (from ¹ May to ³⁰
213 September) and nongrowing season (from ¹ October to ³⁰ April) at specific locations.

214 To directly compare the different effects of permafrost conditions on plant community traits
215 under climate warming, we used the observed ALT time trends (from 1975 to 2017), and the 14
216 study locations were split into two groups. Group A consisted of TSH, QSH, SQH, GZ, MA, WQ,
217 ZAD, XD, ZD, and HSX, with significantly positive increasing trends (ALT significantly increased
218 with time under climate warming). Group B consisted of AD and BLH without significant
219 changes and KXL and QML with significantly negative trends (ALT significantly decreased with
220 time under climate warming). To test whether the split standard was not an artifact of our
221 group method, we applied a control plot and fitted it by linear least squares. The slope was
222 85.88, the correlation coefficient (r^2) was 0.8, and $p < 0.01$, which demonstrated the sensitivity
223 of the changes in ALT in air temperatures.

224 **SI.1.8 Characterizing trends in climate and permafrost**

225 For each location, we calculated the mean ALT, mean soil temperature at 0-50 cm, mean soil
226 temperature at 50-100 cm, mean soil moisture at 0-50 cm, and mean soil moisture at 50-100
227 cm in a given year for our defined growing season to obtain a mean annual value. These
228 variables and the mean annual air temperature for each location were then used to calculate 1)
229 the long-term trends for climate change, active layer warming, active layer moisture, and
230 permafrost thawing and 2) group level (group A and group B) mean annual soil temperature at
231 0-50 cm, soil temperature at 50-100 cm, soil moisture at 0-50 cm, soil moisture at 50-100 cm

232 and variation in ALT. The difference between group A and group B was tested by a *t test*, and
233 the significance level was 0.05. All time intervals were calculated using the Mann–Kendall test
234 (trend package, R 4.1). We excluded datasets that had < 10 years. The control plots that
235 measures the rate of air temperature per decade ($\delta T_{air}/\text{decade}$) and the rate of ALT per
236 decade ($\delta \text{ALT}/\text{decade}$) were used to assess the sensitivity of permafrost thawing to climate
237 warming and fitted by the linear least-squares method. The significance level was $p < 0.05$, and
238 the confidence level was 95%.

239 **SI.1.9 Characterizing trends in soil properties and soil nutrition**

240 We calculated the mean soil bulk density, SOC concentration, TN concentration, C/N, Cl⁻
241 concentration, NO₃⁻-N concentration, NH₄⁺-N concentration, Na⁺ concentration, Ca⁺
242 concentration, and Mg⁺ concentration. For each location, we calculated the mean of the above
243 properties for soil profiles (0-50 cm, 50-100 cm, and 100 cm permafrost front) in a given year to
244 obtain a mean annual value. The definition for the 100 cm permafrost front, as it is not possible
245 to precisely judge or distinguish by eye in the field, was the 100 cm permafrost front soil core
246 that included 5~10 cm permafrost. Mean annual soil properties and soil nutrition were then
247 used to calculate 1) the long-term trends for the 0-50 cm, 50-100 cm and 100 cm permafrost
248 fronts and 2) the variation in soil properties and soil nutrition for group A and group B. The
249 difference between group A and group B was tested by a *t test*, and the significance level was
250 0.05. All trends were calculated by linear regression, and the slope was estimated by the linear
251 least-squares method. The significance level was $p < 0.05$, and the confidence level was 95%.

252 **SI.1.10 Characterizing trends in plant traits**

253 For each location, we calculated the mean plant coverage, aboveground biomass in September,
254 root maximum length, mean plant height (September), and plant community species richness in
255 a given year (in our defined growing season period) to obtain a mean annual value. These
256 variables were then used to 1) calculate the long-term trends for individual locations and 2)
257 calculate the group-level plant trait time trend for group A and group B. All trends were
258 calculated using linear regression and fitted by the least-squares method; the significance level
259 was $p < 0.05$, and the confidence level was 95%.

260

261 **SI.1.11 Linkage between permafrost thawing and nitrogen release**

262 At ambient sites, linear regression was used to identify 1) the nitrogen source that was the
263 major contributor to the 50-100 cm NO_3^- concentration variation, as we hypothesized that 0–50
264 cm was a proxy for the nitrogen source from active layer warming and 93% SOC was attributed
265 to the 0-50 cm and 100 cm permafrost front proxies for the nitrogen source from permafrost
266 thawing, and 2) the relationship between the variation in the NO_3^- concentration within the
267 active layer (0-50 cm, 50-100 cm, and 100-permafrost front) and permafrost thawing (variation
268 in ALT). The r^2 and significance level were calculated by the least-squares method. The
269 significance level was $p < 0.05$, and the confidence level was 95%.

270 To assess the robustness of the inferred enhancement in NO_3^- concentration within the active
271 layer from permafrost thawing, we used a contour map to delineate the variation in nitrate
272 concentration (NO_3^-) within the active layer with permafrost thawing change (variation in ALT)
273 from 1995 to 2017 (SF 15; Surfer 12.0). Kriging was used to grid NO_3^- concentration data at 10
274 cm intervals within 0-500 cm during 1995 to 2007; x axis is year, y axis is depth of active layer, Z
275 axis is NO_3^- , Z axis is linear, there is no transform and inflate conveys hull by 0.

276 **SI.1.12 Causality analysis between maximum root length and nitrogen increase at 50-100 cm**

277 To demonstrate the causal relationship between the maximum root length increase and the
278 nitrogen concentration increase of 50-100 cm, we ran the causality test by convergent cross
279 mapping with the rEDM package of R 4.1. The optimal value of the embedding dimension E was
280 2, estimated by the function of the SSR pred boot. Convergent cross mapping demonstrated
281 that an increase in soil nitrogen of 50-100 cm caused the maximum root length change
282 (increasing), and the time lag was approximately 2 years. This result was consistent with field
283 observations of isotope ^{15}N where labeled N rejected to the front of permafrost could be taken
284 up by the deep-rooted plant in two years. Furthermore, convergent cross mapping was used to
285 improve our understanding of the relationship between climate change or permafrost thawing
286 or active layer warming or active layer soil moisture and maximum root length. The results
287 were assessed by the r^2 and p value, with a significance level <0.05 .

288 **SI.1.13 Multiple regression analysis of drivers of plant trait trends**

289 We conducted a multiple regression analysis of the air temperature, total precipitation, active
290 layer temperature, active layer moisture, variation in ALT, soil nitrogen variation within the
291 active layer (variation in N-NO_3^- concentration and N-NH_4^+ concentration), and drivers of
292 observed plant trait (maximum root length, species richness, and aboveground biomass in
293 September) trends at each location. Predictors in the analysis included growing season air
294 temperature, growing season total precipitation, growing season soil temperature of 0-50 cm,
295 growing season soil temperature at 50-100 cm, growing season soil moisture at 0-50 cm,
296 growing season soil moisture at 50-100 cm, growing season soil nitrogen (including N-NO_3^- and
297 N-NH_4^+) at 0-50 cm, growing season soil nitrogen at 50-100 cm, growing season soil nitrogen at
298 the 100 cm permafrost front, variation in ALT, nongrowing season air temperature, nongrowing
299 season soil temperature at 0-50 cm, nongrowing season soil temperature at 50-100 cm, annual
300 air temperature, annual soil temperature at 0-50 cm, and annual soil temperature at 50-100
301 cm.

302 All variables were standardized by Z-scores to facilitate a comparison of model coefficients
303 across the variables with different units. Selection variables were entered stepwise. We verified
304 that multicollinearity was not a problem by checking that the variance inflation factor was well
305 below ten for all variables (14). We used the leaps R package to select subset models including
306 all predictors and two-way interactions and selected the fitted model having the lowest Akaike
307 information criterion (AIC). The results are described by the coefficient (r^2) and p value, and the
308 significance level <0.05 .

309 **SI.1.14 Structure equation model (SEM)**

310 Piecewise SEM was examined to identify 1) the pathway through which climate change
311 potentially affects plant growth and 2) the difference between the direct and indirect effects of
312 temperature, water balance and soil nutrition on plant growth. The mean value at the site level
313 for the growing season was used in the SEM analysis and split into two groups, A and B
314 (supplementary Fig. S1). Variables that only demonstrated a significant correlation ($p<0.05$)
315 with plant traits in the multiple regression analysis were pooled into the SEM. Nutrition
316 variation was represented by the nitrogen variation, whereas ammonium (NH_4^+) variation

317 delineated the nitrogen released from the permafrost. Ultimately, 7 variables were used in the
318 SEM.

319 All variables were standardized (mean zero, unit variance) using Z-scores. Then, principal
320 component analysis (PCA) was used to summarize the structure between plant growth and
321 driver parameters. We assumed linear Gaussian relationships between variables included in the
322 model, which tested normality with density plots for each variable (15).

323 As plant uptake of nitrogen released from permafrost has a two-year time lag, the final climate
324 change and plant trait dataset was from 1997 to 2017, and the soil nitrogen dataset was from
325 1995 to 2015. We fit separate models window-by-window from 0 to 5 years both for the
326 growing season and nongrowing season to 1) test whether the time lag of 2 years in the SEM
327 was not an artifact setting and 2) account for possible time lag effects of climate change
328 variables (i.e., nongrowing season air temperature and soil temperature) and nitrogen released
329 from the permafrost thawing front during plant aboveground senescence.

330 To examine pathways by which climate change potentially affects plant growth and to
331 differentiate between direct and indirect effects of temperature (air temperature, growing
332 degree days, soil temperature at 0-50 cm, soil temperature at 50-100 cm, and variation in ALT),
333 water balance (soil moisture at 0-50 cm and soil moisture at 50-100 cm) and soil nutrition (N-
334 NO_3^- and N- NH_4^+ concentration in that 0-50 cm, 50-100 cm, and 100 cm-permafrost front) on
335 plant growth, we used piecewise SEMs.

336 Before the SEM analysis, all variables for the 14 locations were 1) split into two groups based on
337 the variation in ALT under climate warming, and the details are presented in Supplementary
338 Fig. S1 and 2) only demonstrated a significant correlation with plant traits ($p < 0.05$) in the above
339 multiple regression analysis and were pooled into the SEM. For each group of variables, the
340 mean value at the level of location was used in SEM analysis. As the plant uptake of nitrogen
341 released from permafrost has a two-year time lag, the final climate change and plant trait
342 dataset was from 1997 to 2017, and the soil nitrogen dataset consisted was from 1995 to 2015.
343 Then, we used maximum likelihood estimation to interpolate the deficiency of data (16).
344 Considering regional climate and using a priori knowledge, we included only growing season

345 climate variables in our SEM, and nongrowing season and annual climate variables were
346 excluded from the analyses. Although plant growth relationships with dormant season climate
347 are occasionally reported, this information was not included in the SEM analyses.

348 After the data were compiled, a conceptual model was constructed to investigate complex (i.e.,
349 direct and indirect) relationships among plant growth and temperature, water balance, and soil
350 nitrogen of both groups of responders. Soil moisture at 0-100 cm was used as a surrogate for
351 the water balance among precipitation, ice melt, unfrozen water, and evaporation in the
352 model. Because the maximum root length ranged from 50 cm to 100 cm for group A, the soil
353 moisture and soil temperature at 0-100 cm were both chosen. For group B, the maximum root
354 length ranged from 0 cm to 50 cm, and the soil moisture and soil temperature both ranged
355 from 0-50 cm. To explore the potential mechanisms behind plant growth responses associated
356 with changes in temperature, moisture and nutrition, the same SEM structure variables were
357 applied to groups A and B.

358 As the nitrogen variation was mainly caused by active layer warming and permafrost thawing,
359 we grouped the variation in nitrogen into two parts: 1) one part was related to active layer
360 warming, as the ammonium (NH_4^+) data were sampled from 2008 to 2017 and nitrate (NO_3^-)
361 data were sampled from 1995 to 2017, the nitrate (NO_3^-) variation at 0-100 cm accounted for
362 73% of the total nitrogen variation at 0-100 cm, and to avoid the uncertainty in data weight,
363 here only the nitrate (NO_3^-) concentration in the 0–100 cm (averaged by NO_3^- concentrations at
364 0–50 cm and 50–100 cm) layer was used for further analysis with the data on the ammonium
365 (NH_4^+) concentration in the 0–100 cm layer being excluded; 2) the other part was related to
366 permafrost thawing. NH_4^+ variation accounted for 93% of the nitrogen variation in the 100 cm
367 permafrost front. To avoid uncertainty in data weight, only the ammonium (NH_4^+) variation was
368 included to delineate the nitrogen released from permafrost.

369 In the end, 7 variables were used in the SEM: (1) the mean air temperature (MAT) during the
370 plant growing season; (2) the mean soil water content at 0–100 cm (SWC; averaged by 0–50
371 and 50-100 cm) during the growing season; (3) growing degree days, which is a cumulative sum
372 of daily air temperature above 0 °C; (4) active layer warming, which was proxied by the mean

373 soil temperature of 0–100 cm (T_{soil} ; averaged by soil temperature at 0–50 and 50–100 cm) and
374 NO_3^- concentration at 0–100 cm; (5) permafrost thawing, which was proxied by the maximum
375 ALT and NH_4^+ concentration of the 100 cm–permafrost front; (6) plant growth, including
376 aboveground biomass in September and species richness; and (7) the maximum length of roots,
377 which was the maximum root depth.

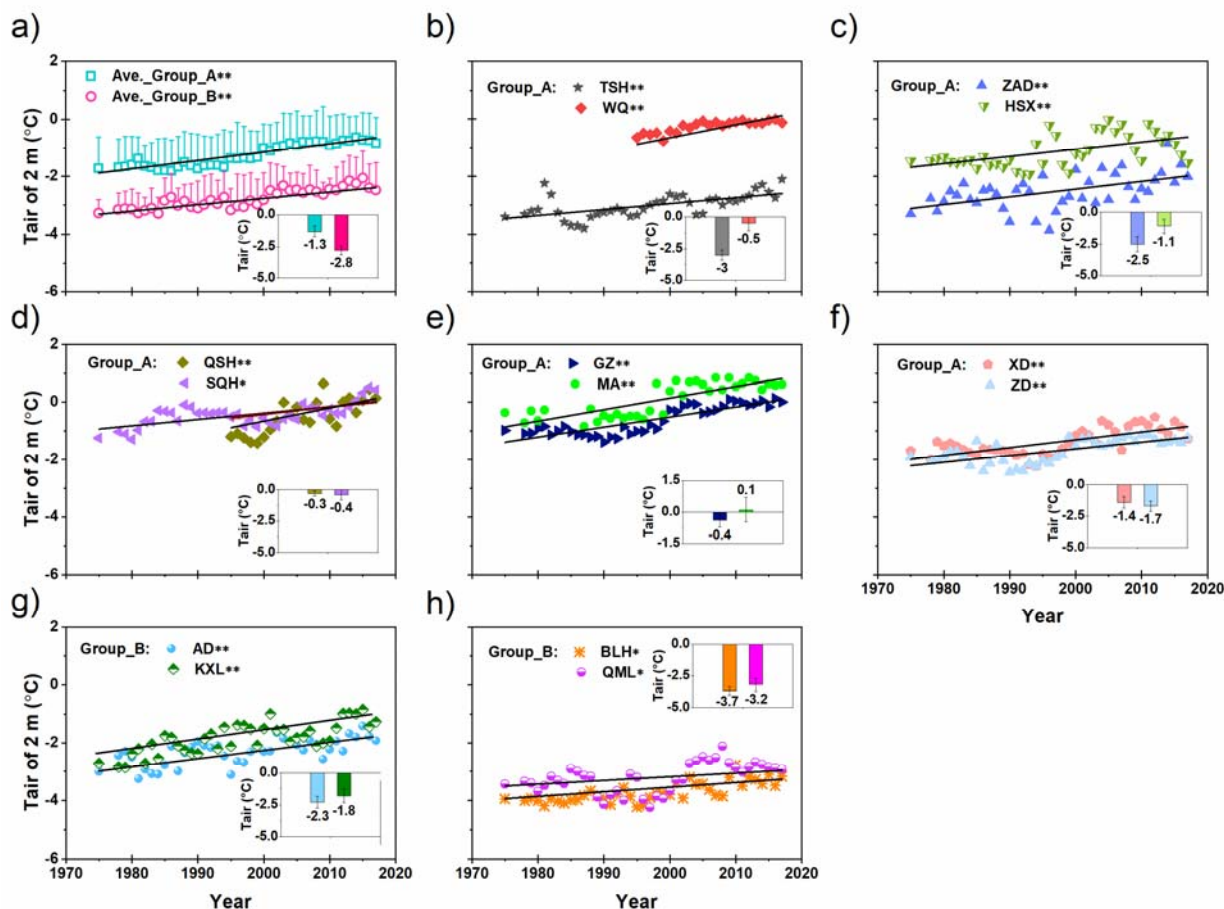
378 To test whether the time lag (2 years) in the SEM was not an artifact and account for possible
379 time lag effects of climate change variables (i.e., nongrowing season air temperature and soil
380 temperature) and the nitrogen released from the permafrost thawing front when plants
381 experienced aboveground senescence, we fit separate models window-by-window from 0 to 5
382 years both for the growing season and nongrowing season.

383 We then created an expression of community structure compatible with the SEM. We assumed
384 linear Gaussian relationships between the variables included in the model that tested each
385 variable for normality with density plots. All variables were standardized (mean zero, unit
386 variance) using Z-scores. Then, PCA was used to summarize the structure between plant growth
387 and climate drivers by FactoMineR packages of R 4.1. All variables were entered before SEM
388 analysis to facilitate the interpretation of parameter estimates.

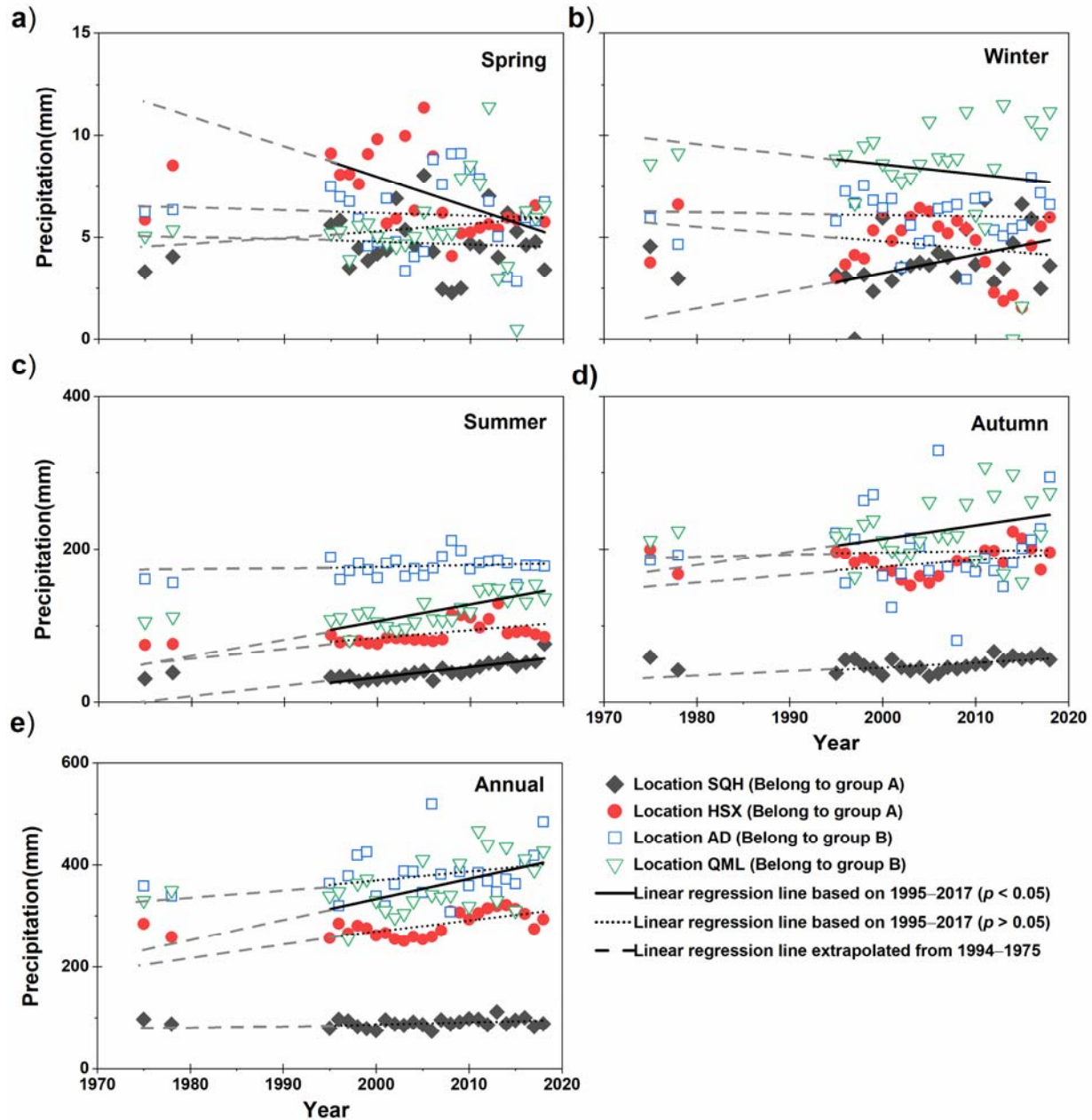
389 To test the goodness-of-fit of our SEMs, we used chi square (χ^2), degrees of freedom (*d.f.*),
390 and the root-mean-square error of approximation (RMSEA; the model had a good fit when the
391 RMSEA was indistinguishable from zero to 0.05). A path coefficient is analogous to the partial r^2
392 or regression weight and describes the strength and sign of the relationships between two
393 variables (16). We calculated the standardized total effects of all drivers on the plant growth of
394 active layer warming and permafrost thawing attributes. The net influence that one variable
395 had upon another was calculated by summing all direct and indirect pathways (effects)
396 between two variables. All SEM analyses were conducted using the piecewise SEM package of R
397 4.1.

398

399



401
 402 **Supplementary Figure S1.** Temporal changes in annual air temperature (Tair) at a height of 2 m
 403 (MAAT) on the Tibetan Plateau from 1975 to 2017. **a** is shown MAAT temporal changes for
 404 group A locations and group B locations from 1975 to 2017. For group A and B separation
 405 details, please see Supplementary Figure S1. Error bars denote SE, $n = 8$ for 1975–1994 and $n =$
 406 10 for 1995–2017 for group A, and $n=4$ for group B. Subfigures **b**, **c**, **d**, **e**), and **f** show the
 407 annual air temperature data of group A locations of TSH, WQ, ZAD, HSX, QSH, SQH, GZ,
 408 MA, XD, and ZD, respectively. Subfigures **g** and **h** show the annual air temperature data of
 409 group B locations of AD, KXL, and BLH, QML, respectively. Solid lines for 1975–2017
 410 indicate significant changes ($p < 0.01$, **; $p < 0.05$, *). The insets show the mean annual air
 411 temperature (MAAT) for group A, group B and specific locations, which with different color
 412 columns from 1975 (locations WQ and QSH from 1995) to 2017.

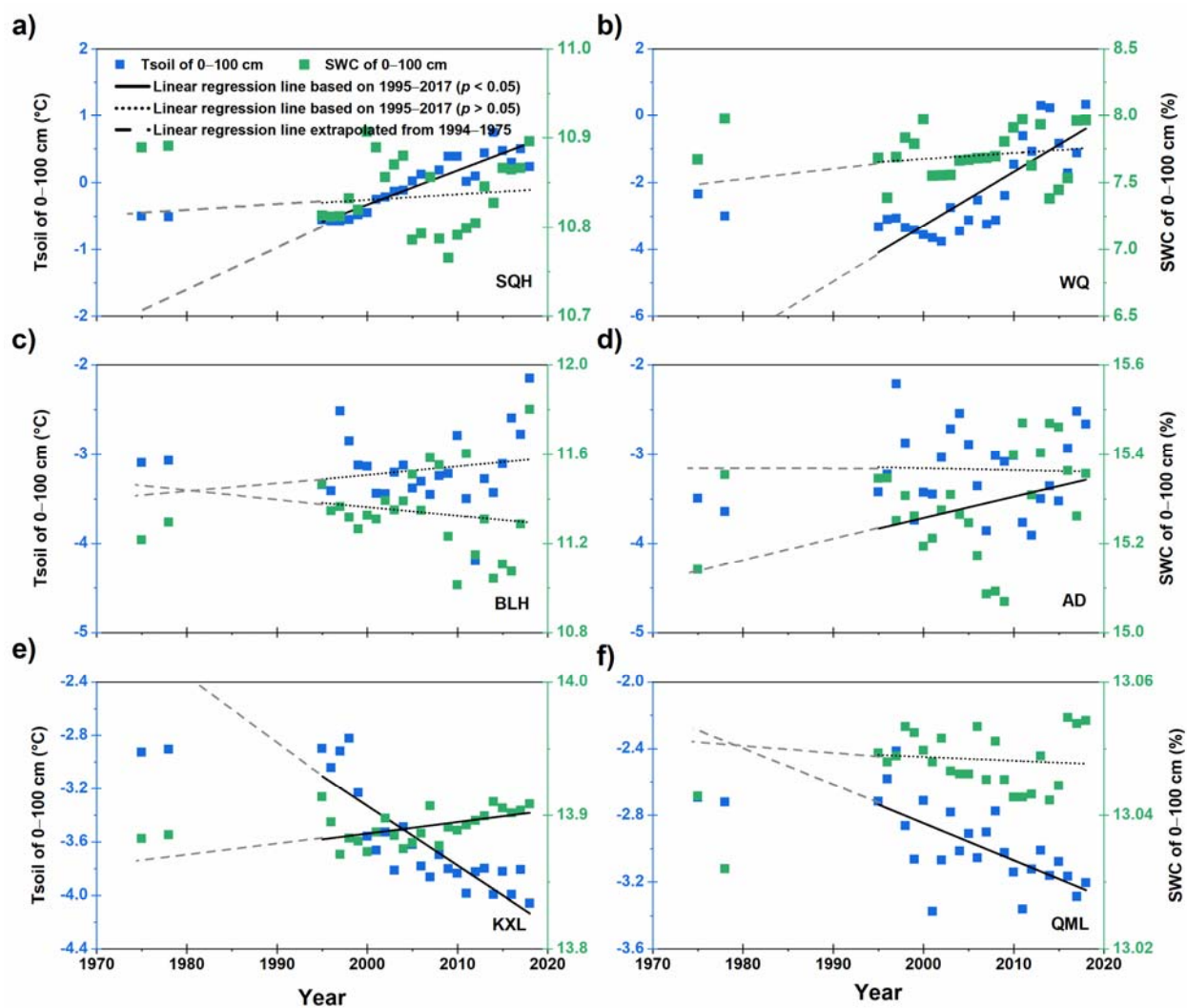


413

414 **Supplementary Figure S2.** Precipitation of 4 representative types of 14 locations (locations
 415 SQH and HSX belonged to the Group A; Locations AD and QML belonged to the Group B) in
 416 the permafrost region of the Tibetan Plateau from 1975 to 2017. Subfigure **a**, **b**, **c**, **d**, and **e** is
 417 used to designate spring, winter, summer, autumn, and annual total precipitation, respectively.

418

419

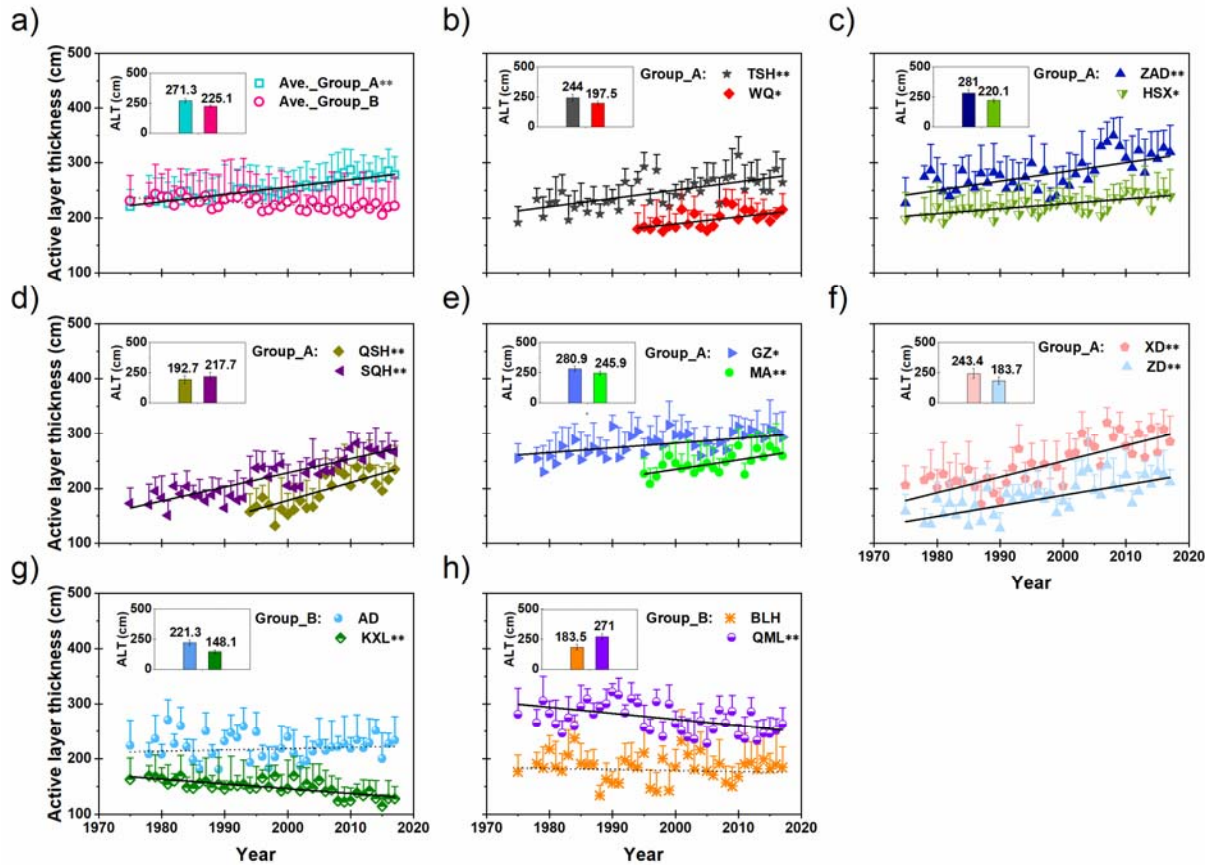


421

422 **Supplementary Figure S3.** Mean annual soil temperature (Tsoil) and soil water content (SWC)

423 of 0–100 cm changes from 1975–2017 for six type locations on Tibetan plateau (Figs. S9 a-f).

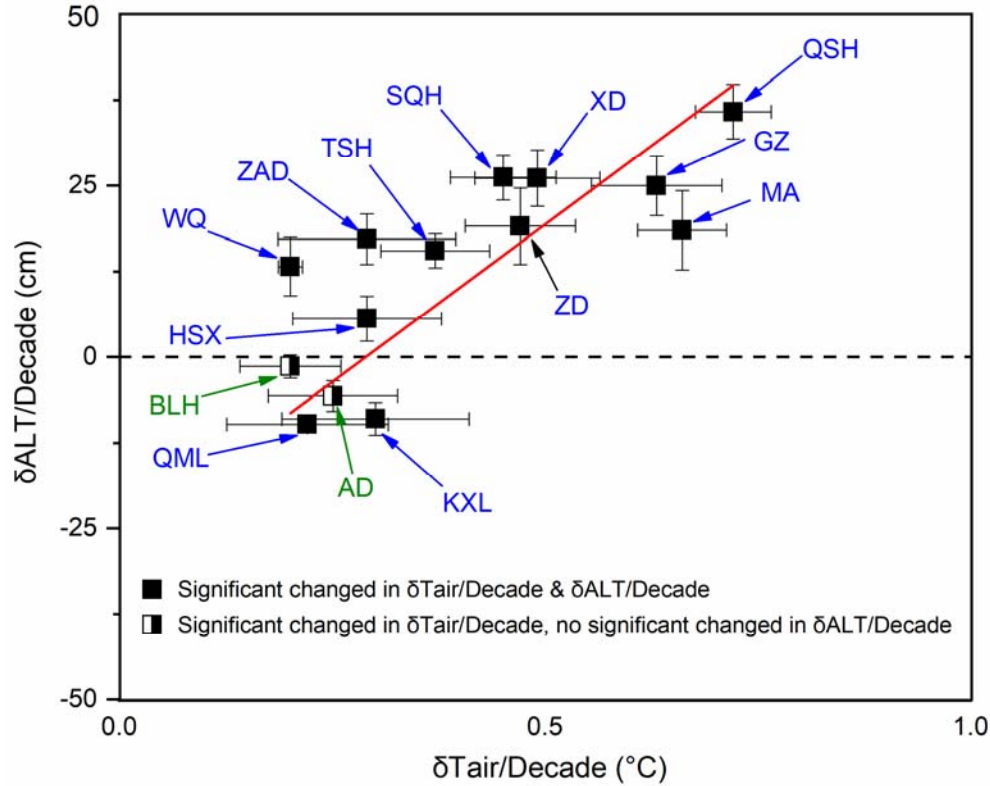
424 Location SQH, WQ belonged to group A; location BLH, AD, KXL, QML belonged to group B.



425 **Supplementary Figure S4.** Temporal changes in active layer thickness (ALT) on the Tibetan
 426 Plateau from 1975 to 2017. **a** is shown mean ALT temporal changes for group A locations and
 427 group B locations from 1975 to 2017. Error bars denote SE, $n = 7$ for 1975–1994 and $n = 10$ for
 428 1995–2017 for group A, and $n=4$ for group B. Subfigures **b**, **c**, **d**, **e**, and **f** show the ALT data of
 429 group A locations of TSH, WQ, ZAD, HSX, QSH, SQH, GZ, MA, XD, and ZD, respectively.
 430 Subfigures **g**) and **h**) show the ALT data of group B locations of AD, KXL and BLH, QML,
 431 respectively. Solid lines for 1975–2017 indicate significant changes ($p < 0.01$, ** and $p < 0.05$,
 432 *), while dotted lines indicate non-significant changes ($p > 0.05$). The insets show the mean
 433 annual ALT for group A, group B and specific locations, which with different color columns
 434 from 1975 (locations WQ, QSH, and MA from 1995) to 2017.

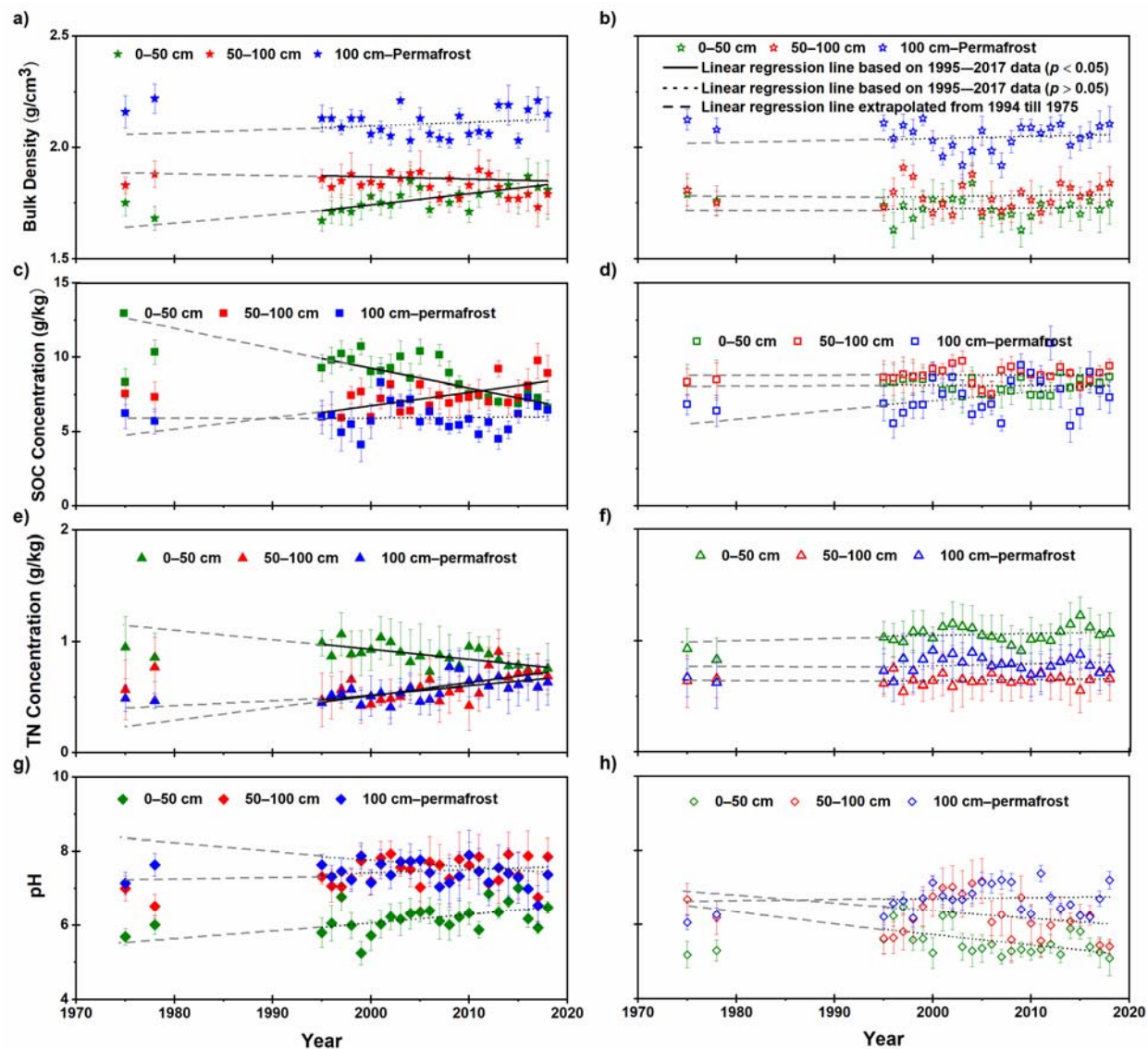
435

436



437

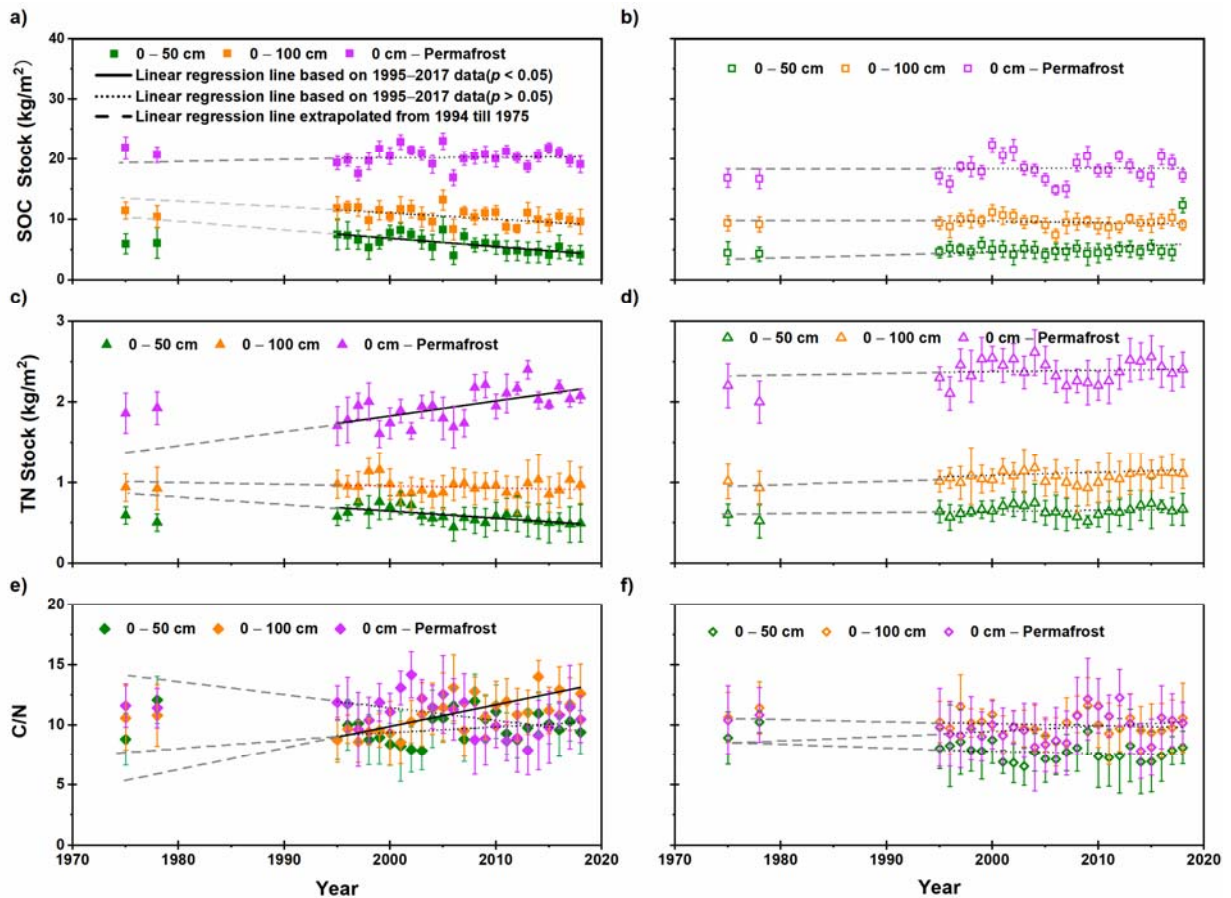
438 **Supplementary Figure S5.** Changes in air temperature and active layer thickness (ALT) per
 439 decade on the Tibetan Plateau from 1975 to 2017. Based on location-specific *t*-tests, the 14
 440 stations are divided in group A locations (with a significant positive change in ALT with respect
 441 to air temperature; locations TSH, QSH, SQH, GZ, WQ, ZAD, XD, ZD, and HSX) and group B
 442 locations (with a significant negative in ALT with respect to air temperature, locations KXL and
 443 QML or no significant in ALT with respect to air temperature, locations AD and BLH). One
 444 standard deviation is shown as horizontal and vertical bars for $\delta T_{air}/decade$ ($n = 4$) and
 445 $\delta ALT/decade$ ($n = 4$), respectively. The red line is the linear fit line, which illustrates the
 446 sensitivity of changes in active layer thickness and changes in air temperatures ($y = 85.88x -$
 447 $25.02, r = 0.80; p < 0.01$).



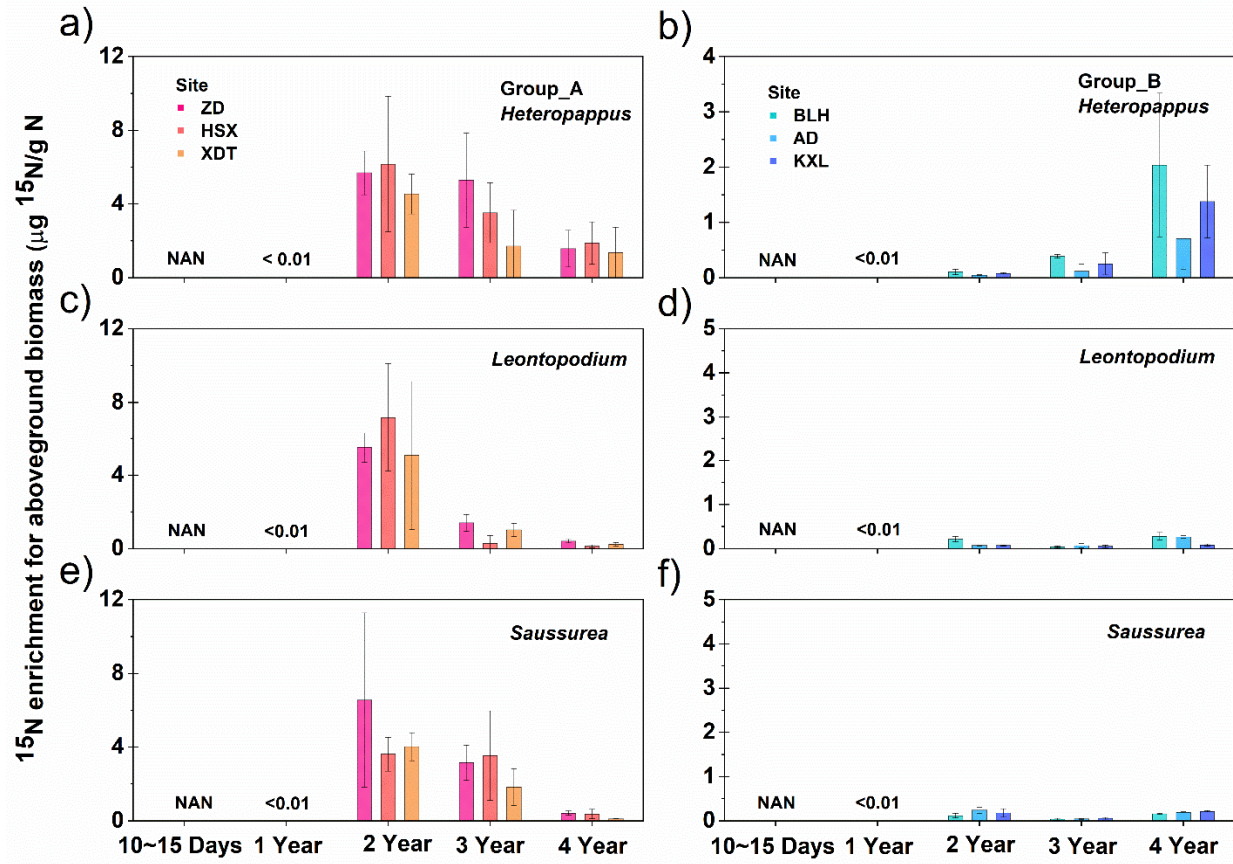
448

449 **Supplementary Figure S6.** Temporal changes in soil properties at three depth intervals
 450 averaged at locations across the Tibetan Plateau, which include soil bulk density, soil organic
 451 carbon (SOC) concentration, total nitrogen (TN) concentration, and soil pH. Average data are
 452 shown for group A locations (subfigures **a**, **c**, **e**, and **g**) and group B locations (subfigures **b**, **d**, **f**
 453 and **h**). Vertical bars represent one standard deviation, $n = 6$ for 1975, 1978, and $n = 10$ for
 454 1995–2017 in group A; $n = 3$ for 1975, 1978 and $n = 4$ for 1995–2017 in group B.

455



456 **Supplementary Figure S7.** Temporal changes in the soil organic carbon stock (SOC stock),
 457 total nitrogen stock (TN stock), and carbon-to-nitrogen ratio (C/N) at three depth intervals at
 458 locations across the Tibetan Plateau. Subfigures **a**, **c**, and **e** for group A locations; **b**, **d**, and **f** for
 459 group B locations. Worth notes, three depth intervals were 0–50 cm, 0–100 cm, and 0 cm–
 460 permafrost. Vertical bars represent one standard deviation, $n = 6$ for 1975, 1978, and $n = 10$ for
 461 1995–2017 in group A; $n = 3$ for 1975, 1978 and $n = 4$ for 1995–2017 in group B.



462

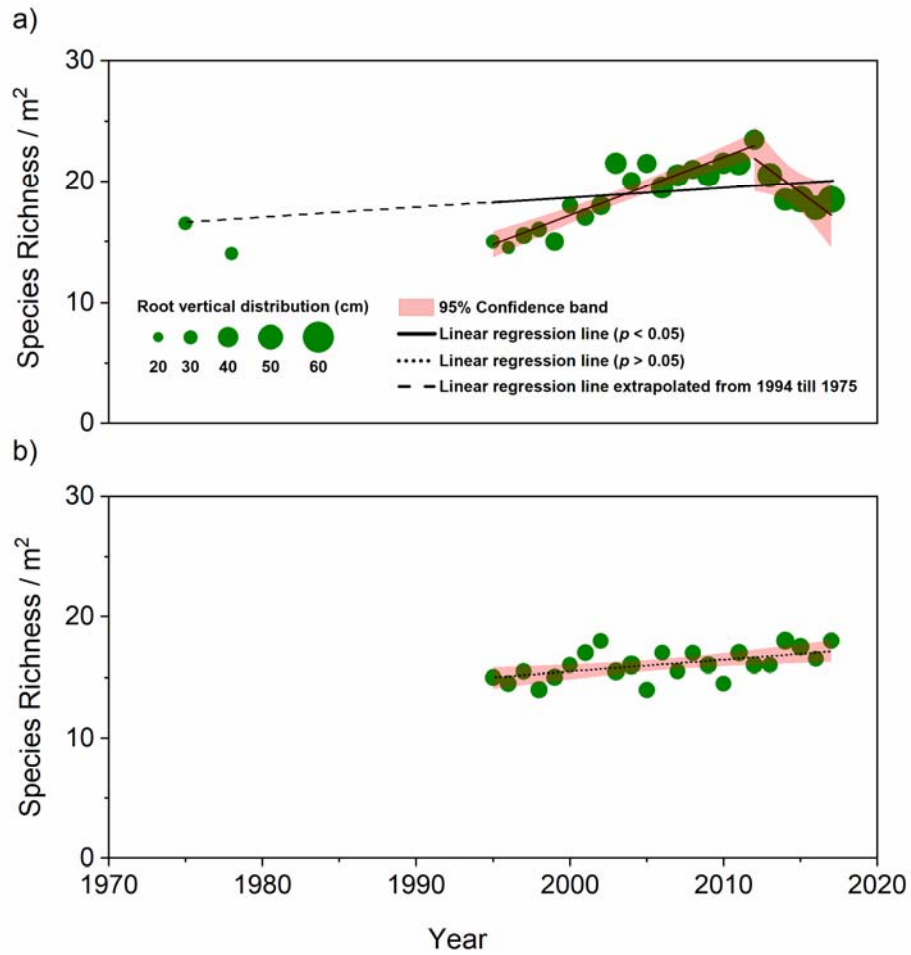
463 **Supplementary Figure S8** Enrichment $^{15}\text{N}_{\text{NH}_4\text{Cl}}$ in aboveground mass (including leaves and
 464 stem) of shallow-rooted species (average root length less than 20 cm) by treatment after
 465 10~15days, 1 year, 2 years, 3 years, and 4 years for group A (a, c, e) and group B (b, d, f). a and
 466 b were *Heteropappus bowerii* (Hemsl.) Griens. (*Heteropappus*), c and d were *Leontopodium*
 467 *nanum* (Hook. f. et Thoms.) Hand.-Ma (*Leontopodium*), and e and f were *Saussurea arenaria*
 468 Maxim (*Saussurea*). vertical bars representing one standard deviation, n = 15, excluded the 1
 469 year, n= 12.

470

471

472

473

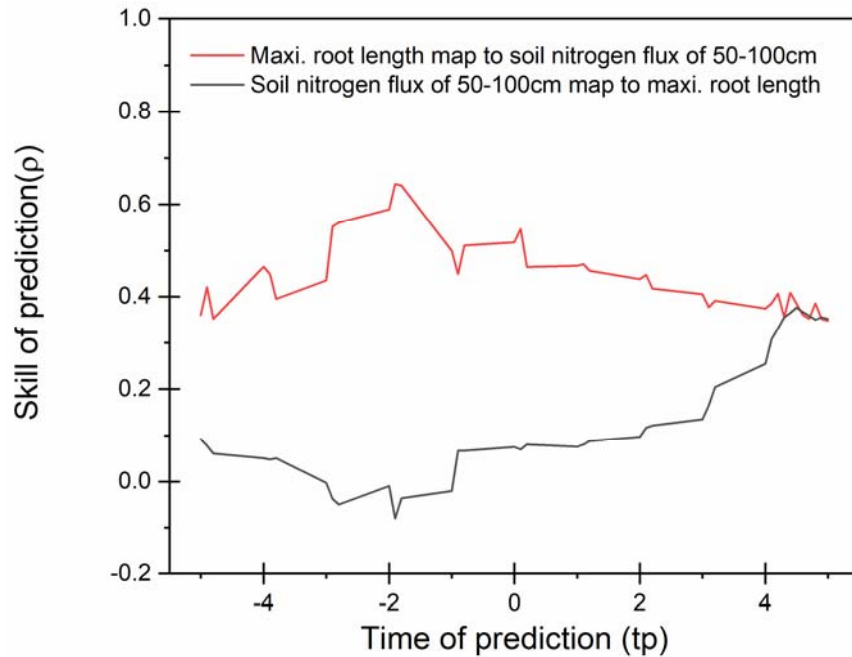


474

475 **Supplementary Figure S9.** Changes in specie richness and root vertical distribution from 1975
 476 to 2017. The size of green dot indicates the difference of root vertical distribution. Subfigure **a**
 477 show the group A locations and **b** for the group B locations.

478

479



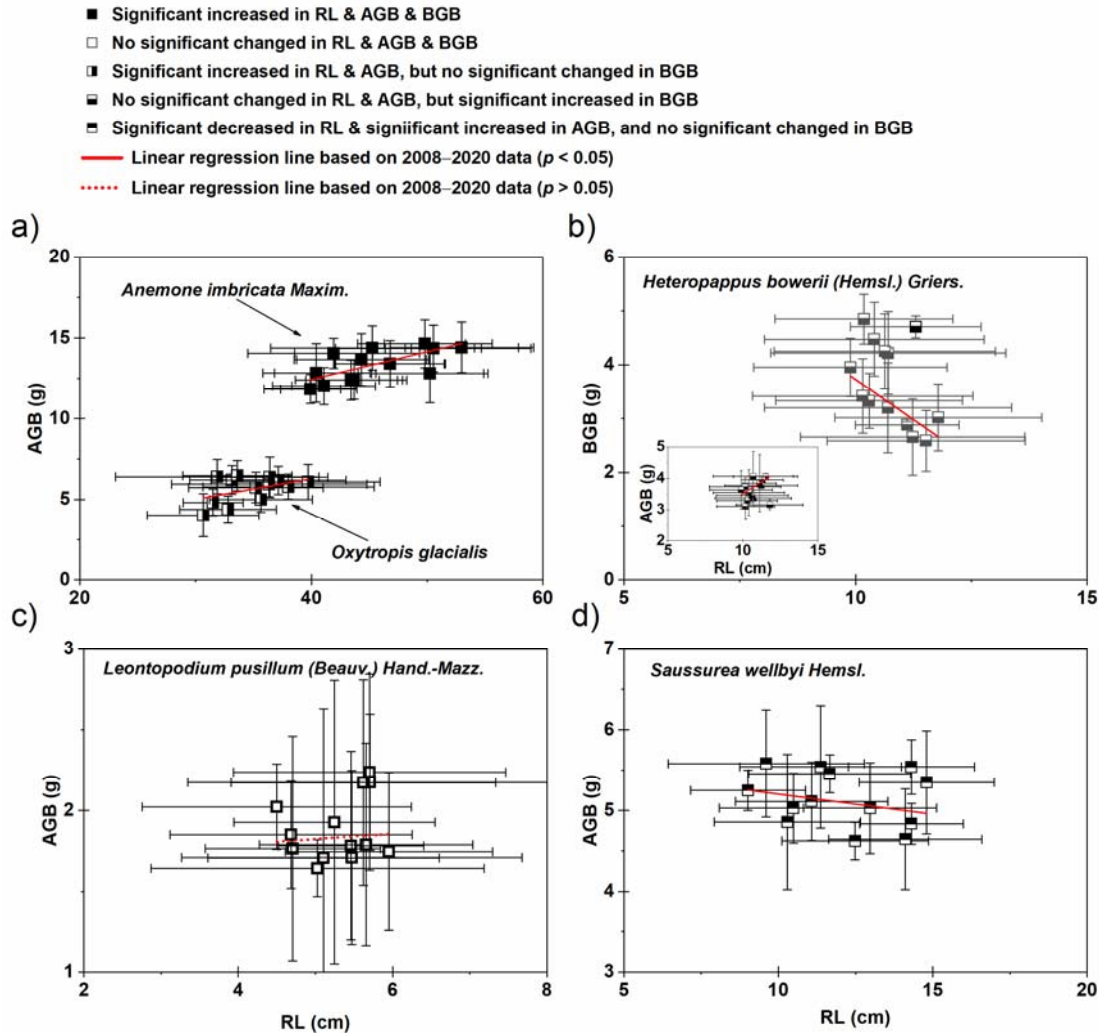
480

481 **Supplementary Figure S10.** Causality test running for the variation of root length map to soil
 482 nitrogen flux of 50-100 cm (red line) and soil nitrogen flux of 50-100 cm map to root length
 483 (grey line), respectively. Skill of prediction (ρ) for red line reaches the peak when time
 484 prediction (tp) around -2, demonstrate that the soil nitrogen flux of 50cm caused the root length
 485 change (increase), and the time lag is about 2 years. This result consisted with field observations
 486 of isotope ^{15}N that label N rejected to the front of permafrost is could be uptake by the deep-
 487 rooted plant in two years. In contrast, ρ of the grey line peak *arrived* maximum when tp around
 488 4, which means the hypothesis of variation of root length caused soi nitrogen flux of 50cm
 489 variation is impossible. The optimal value of the embedding dimension $E=2$, estimated by
 490 function of SSR pred boot (R).

491

492

493

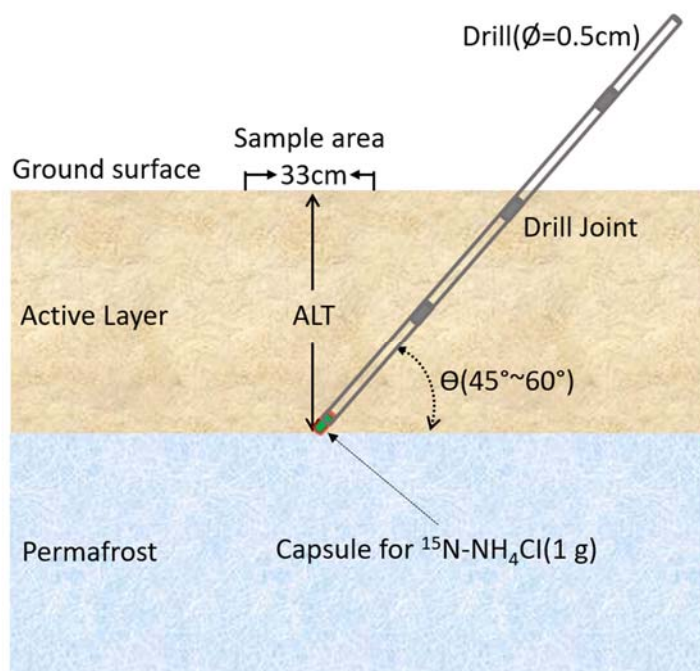


494

495 **Supplementary Figure S11.** Changes in root length (RL), aboveground biomass (AGB), and
 496 belowground biomass (BGB) for species type at the location XD (belonging for group A) from
 497 2008 to 2020. **a** is two types deep-rooted species *Anemone imbricata Maxim.* and *Oxytropis*
 498 *glacialis*; **b**, **c**, and **d** are three shallow-rooted species *Leontopodium pusillum (Beauv.) Hand.-*
 499 *Mazz.*, *Heteropappus bowerii (Hemsl.) Griens.*, and *Saussurea wellbyi Hemsl.* **Worth note**, **b** is
 500 the changes in RL and BGB, the **inset** is the changes in RL and AGB for *Heteropappus bowerii*
 501 (Hemsl.) Griens. Vertical and horizontal bars represent one standard deviation, $n = 4$.

502

503



504

505 **Supplementary Figure S12.** Schematic of field experiment for $^{15}\text{N-NH}_4\text{Cl}$ capsule rejection to
506 the front of permafrost. Collection of plants were made only immediately above the rejection
507 point. Tests have been made previous (11) to document that the method ensure that residue is not
508 left at shallow depth which otherwise might be accessible for plant roots.

509

510

511

512

513

514 **Supplementary Table ST1.** Species abundance or species turnover (presence or absence) over time of group A.

| No. | HP (cm) | RL (cm) | Year | | | | | | | | | | | | | | | | | | | | | | | | |
|-----|------------|------------|----------|----------|----------|----------|----------|----------|----------|----------|----------|----------|----------|----------|----------|----------|----------|----------|----------|----------|----------|----------|----------|----------|----------|----------|----------|
| | | | 19 75 | 19 78 | 19 95 | 19 96 | 19 97 | 19 98 | 19 99 | 20 00 | 20 01 | 20 02 | 20 03 | 20 04 | 20 05 | 20 06 | 20 07 | 20 08 | 20 09 | 20 10 | 20 11 | 20 12 | 20 13 | 20 14 | 20 15 | 20 16 | 20 17 |
| 1 | 27.4 | 37.2 | √ | √ | √ | √ | √ | √ | √ | √ | √ | √ | √ | √ | | √ | √ | √ | √ | | √ | √ | | √ | √ | √ | |
| 2 | 27.4 | 38.2 | √ | √ | √ | √ | √ | √ | √ | √ | √ | √ | √ | √ | √ | | | | √ | | | √ | | | | | |
| 3 | 34.8 | 40.2 | √ | √ | √ | √ | √ | √ | √ | √ | √ | √ | √ | √ | √ | | | | | √ | √ | √ | √ | | | | |
| 4 | 26.5 | 33.5 | √ | √ | √ | √ | √ | √ | √ | √ | √ | √ | √ | √ | √ | √ | √ | √ | √ | √ | √ | √ | √ | | √ | √ | |
| 5 | 18.3 | 23.5 | √ | √ | √ | | √ | √ | | √ | √ | | √ | √ | √ | | | | | | | | √ | √ | | | |
| 6 | 15.4 | 18.5 | √ | √ | √ | √ | √ | √ | √ | √ | √ | √ | √ | √ | √ | √ | √ | √ | √ | √ | √ | √ | √ | √ | √ | √ | |
| 7 | 23.6 | 38.2 | √ | √ | √ | √ | √ | √ | √ | √ | √ | √ | √ | √ | | √ | √ | √ | | | | | | | | | |
| 8 | 6.5 | 14.0 | √ | √ | √ | √ | | √ | √ | | √ | √ | √ | √ | √ | | | | | | √ | √ | | | | | |
| 9 | 2.8 | 29.9 | √ | √ | √ | √ | √ | √ | √ | √ | √ | √ | √ | √ | | | | | √ | √ | | | | | | | |
| 10 | 1.8 | 23.7 | √ | √ | √ | √ | √ | √ | √ | √ | √ | √ | √ | √ | | | √ | √ | √ | √ | | | | | | | |
| 11 | 6.2 | 15.8 | √ | √ | √ | √ | √ | √ | √ | √ | | √ | | √ | | √ | | | | √ | √ | | | | | | |
| 12 | 8.0 | 14.6 | √ | √ | √ | √ | √ | √ | √ | √ | √ | √ | √ | √ | √ | √ | √ | √ | √ | √ | √ | √ | √ | √ | √ | √ | √ |
| 13 | 5.9 | 5.1 | √ | √ | √ | √ | √ | √ | √ | √ | √ | √ | | | | | | | | | | | | | | | |
| 14 | 4.7 | 16.6 | √ | √ | √ | √ | | √ | | | √ | | √ | | √ | | | | | | | | √ | | √ | | |
| 15 | 8.1 | 11.4 | √ | √ | √ | √ | √ | √ | √ | √ | √ | √ | √ | √ | | | | √ | | √ | | | | | | | |
| 16 | 6.5 | 7.3 | √ | √ | | | √ | √ | √ | √ | √ | √ | | | | | | | | | | | | | | | |
| 17 | 6.8 | 13.8 | √ | √ | √ | | √ | | √ | √ | | √ | √ | | | √ | | | | | | | | | | | |
| 18 | 5.4 | 5.2 | √ | √ | √ | √ | √ | √ | √ | √ | √ | √ | | √ | √ | | | | | √ | | | | | | | |
| 19 | 11.1 | 12.1 | √ | √ | | √ | √ | √ | √ | √ | √ | √ | √ | √ | | | √ | √ | | | | | | | | | |
| 20 | 6.3 | 5.5 | √ | √ | √ | √ | | | | √ | | | √ | | √ | | | | | | | | | | | | |
| 21 | 9.8 | 10.8 | √ | √ | √ | √ | √ | √ | √ | √ | √ | √ | | √ | | √ | √ | | | | | | | | | | |
| 22 | 7.8 | 10.6 | √ | √ | √ | √ | √ | √ | √ | √ | √ | √ | √ | √ | √ | √ | √ | √ | √ | | √ | | √ | √ | √ | | |
| 23 | 5.7 | 5.1 | √ | √ | √ | √ | | √ | | √ | | √ | | √ | √ | | | | | | | | | | | | |
| 24 | 7.3 | 6.8 | √ | √ | √ | √ | √ | √ | | √ | √ | √ | | √ | | √ | √ | √ | | | | | | | | | |
| 25 | 6.4 | 6.2 | √ | √ | | √ | √ | √ | √ | √ | √ | √ | | √ | | √ | | | | | | | | | | | |
| 26 | 4.7 | 5.1 | √ | √ | √ | | √ | | √ | √ | √ | | √ | | | | | | | | | | | | | | |

515 **Note** that HP is acronymic of mean height of plant, RL is acronymic of mean root length, values reported as annual means, not show
 516 the standard error. Species presence is used to designate √, species absence is used to designate blank, and No. is used to designate the
 517 species name. 1, *Kobresia littledalei* C. B. Clarke 2, *Kobresia tibetica* Maxim 3, *Kobresia robusta* Maxim 4, *Carex nudicarpa* (Y. C.
 518 Yang) S. R. Zhang (2015) 5, *Triglochin maritimum* 6, *Polygonum viviparum* L. 7, *Astragalus purdomii* 8, *Ranunculus longicaulis* C.
 519 A. Mey. var. *nephelogenes* (Edgew.) L.Liou 9, *Androsace tangulashanensis* Y. C. Yang et R. F. Hua. 10, *Androsace integra* (Maxim.)
 520 Hand - Mazz. 11, *Lagotis brachystachya* Maxim. 12, *Leontopodium pusillum* (Beauv.) Hand.-Mazz. 13, *Primula minor* Balf. f. et
 521 Ward 14, *Saussurea stella* Maxim. 15, *Aster alpinus* L. 16, *Thalictrum alpinum* L. 17, *Oxygraphis glacialis* (Fisch.) Bunge 18,
 522 *Saxifraga unguiculata* Engl. 19, *Taraxacum brevirostre* Hand.-Mazz. 20, *Silene gonosperma* 21, *Saussurea wellbyi* Hemsl. 22,
 523 *Polygonum sibiricum* Laxm. 23, *Gentianopsis paludosa* (Hook. f.) Ma 24, *Gentiana crenulatotruncata* (Marq.) T. N. Ho 25, *Gentiana*
 524 *futtereri* Diels et Gilg 26, *Glaux maritima* L. 27, *Callianthemum pimpinelloides* 28, *Heteropappus bowerii* (Hemsl.) Griens. 29, *Carex*
 525 *parvula* O. Yano 30, *Kobresia deasyi* C. B. Clarke 31, *Taraxacum tibetanum* Hand.-Mazz. 32, *Hedinia tibetica* (Thomson) Ostenf. 33,
 526 *Delphinium candelabrum* Ostf. var. *monanthum* (Hand.-Mazz.) W. T. Wang 34, *Delphinium candelabrum* Ostf.
 527 var. *monanthum* (Hand.-Mazz.) W. T. Wang 35, *Allium cyaneum* Regel 36, *Oxytropis pauciflora* Bunge 37, *Kobresia humilis* (C. A.
 528 Mey. ex Trautv.) Sergiev 38, *Iris potaninii* Maxim. 39, *Saussurea melanotrica* Hand.-Mazz. 40, *Erysimum chamaephyton* Maxim 41,
 529 *Parnassia trinervis* 42, *Corydalis dasyptera* Maxim. 43, *Potentilla multicaulis* Bge. 44, *Potentilla saundersiana* 45, *Arenaria*
 530 *brevipetala* Y. W. Tsui et L. H. Zhou. 46, *Aconitum tanguticum* (Maxim.) Stapf 47, *Dimorphostemon landulosus* Kar. et Kir 48,
 531 *Potentilla bifurca* 49, *Ajania tibetica* 50, *Aster flaccidus* Bge. subsp. *glandulosus* (Keissl.) Onno 51, *Pedicularis cheilanthifolia* 52,
 532 *Cremanthodium humile* 53, *Cortiella caespitosa* Shan et Sheh 54, *Ajania khartensis* 55, *Thylacospermum* Fenzl T. rupifragum
 533 Schrenk. 56, *Ceratoides compacta* (Losinsk.) Tsien et C. G. Ma 57, *Rheum moorcroftianum* Royle 58, *Rhodiola algida* (Ledeb.)
 534 Fisch. et Mey. 59, *Rhodiola quadrifida* 60, *Heraeleum millefolium* 61, *Polygonum sibiricum* Laxm. var. *thomsonii* Meisn. Ex 62,
 535 *Potentilla parvifolia* Fisch. ex. Lehm. 63, *Myricaria prostrata* Hook. f. et Thoms. ex Benth. 64, *Oxytropis glacialis* 65, *Poa*
 536 *litwinowiana* Ovcz. 66, *Elymus nutans* Griseb. 67, *Stipa purpurea* 68, *Dracocephalum heterophyllum* Benth 69, *Allium carolinianum*

537 DC. 70, *Carex orbicularinucis* 71, *Carex moorcroftii* Falc. Ex Boott 72, *Meconopsis horridula* Hook. f. et Thoms. 73, *Anemone*
538 *imbricata* Maxim. 74, *Microula tibetica* 75, *Sibbaldia adpressa* 76, *Pleurospermum hedinii* 77, *Saussurea tibetica* C. Winkl 78,
539 *Saussurea Arenaria* 79, *Oxytropis melanocalyx* Bunge 80, *Trisetum spicatum* 81, *Trisetum tibeticum* P. C. Kuo et Z. L. Wu 82, *Carex*
540 *capillifolia* (Decne.) S. R. Zhang 83, *Draba altaica* (C. A. Mey.) Bunge 84, *Hypocoum erectum* L. 85, *Stipa roborowskyi* Roshev 86,
541 *Oxytropis stracheyana* Benth. ex Baker 87, *Astragalus melanostachys*.

542

543

544

545 **Supplementary Table ST2. Species abundance or species turnover (presence or absence) over time of group B.**

| No. | HP (cm) | RL (cm) | Year | | | | | | | | | | | | | | | | | | | | | | | | |
|-----|------------|------------|----------|----------|----------|----------|----------|----------|----------|----------|----------|----------|----------|----------|----------|----------|----------|----------|----------|----------|----------|----------|----------|----------|----------|----------|----------|
| | | | 19 75 | 19 78 | 19 95 | 19 96 | 19 97 | 19 98 | 19 99 | 20 00 | 20 01 | 20 02 | 20 03 | 20 04 | 20 05 | 20 06 | 20 07 | 20 08 | 20 09 | 20 10 | 20 11 | 20 12 | 20 13 | 20 14 | 20 15 | 20 16 | 20 17 |
| 1 | 30.8 | 37.8 | √ | √ | √ | √ | √ | √ | √ | √ | √ | √ | √ | √ | √ | √ | √ | √ | √ | √ | √ | √ | √ | √ | √ | √ | |
| 2 | 29.3 | 37.0 | √ | √ | √ | √ | √ | √ | √ | √ | √ | √ | √ | √ | √ | √ | √ | √ | √ | √ | √ | √ | √ | √ | √ | √ | √ |
| 3 | 37.7 | 37.2 | √ | √ | √ | √ | √ | √ | √ | √ | √ | √ | √ | √ | √ | √ | √ | √ | √ | √ | √ | √ | √ | √ | √ | √ | √ |
| 4 | 29.7 | 31.6 | √ | √ | √ | √ | √ | √ | √ | √ | √ | √ | √ | √ | √ | √ | √ | √ | √ | √ | √ | √ | √ | √ | √ | √ | √ |
| 5 | 22.3 | 23.0 | √ | √ | √ | √ | √ | | √ | √ | | √ | √ | √ | | √ | √ | √ | √ | | √ | √ | √ | √ | √ | √ | |
| 7 | 26.6 | 33.5 | √ | √ | √ | √ | √ | √ | √ | √ | √ | √ | √ | √ | √ | √ | √ | √ | √ | √ | √ | √ | √ | √ | √ | √ | √ |
| 8 | 11.4 | 14.7 | √ | √ | √ | √ | √ | √ | √ | √ | √ | √ | √ | √ | √ | √ | √ | √ | √ | √ | √ | √ | √ | √ | √ | √ | √ |
| 9 | 8.3 | 28.9 | √ | √ | √ | √ | √ | √ | √ | √ | √ | √ | √ | √ | √ | √ | √ | √ | √ | √ | √ | √ | √ | √ | √ | √ | √ |
| 10 | 6.1 | 25.6 | √ | √ | √ | √ | √ | √ | √ | √ | √ | √ | √ | √ | √ | √ | √ | √ | √ | √ | √ | √ | √ | √ | √ | √ | √ |
| 12 | 13.2 | 16.1 | √ | √ | √ | √ | √ | √ | √ | √ | √ | √ | √ | √ | √ | √ | √ | √ | √ | √ | √ | √ | √ | √ | √ | √ | √ |
| 13 | 9.8 | 9.9 | √ | √ | √ | √ | √ | √ | √ | √ | √ | | | | √ | √ | √ | √ | √ | √ | √ | √ | √ | √ | √ | √ | √ |
| 15 | 12.4 | 12.0 | √ | √ | √ | √ | √ | √ | √ | √ | √ | √ | √ | √ | √ | √ | √ | √ | √ | √ | √ | √ | √ | √ | √ | √ | √ |
| 16 | 10.4 | 8.2 | √ | | | √ | | | | | √ | √ | | | | | | √ | | | | | | √ | √ | √ | √ |
| 17 | 10.8 | 15.0 | √ | √ | √ | √ | √ | √ | √ | √ | √ | √ | √ | √ | √ | √ | √ | √ | √ | √ | √ | √ | √ | √ | √ | √ | √ |
| 18 | 10.4 | 9.4 | √ | | | | | | | | | | | | | | | | | | | | √ | | | | |
| 19 | 15.9 | 16.0 | √ | √ | √ | √ | √ | √ | √ | √ | √ | √ | √ | √ | √ | √ | √ | √ | √ | √ | √ | √ | √ | √ | √ | √ | √ |
| 20 | 12.3 | 8.1 | √ | | | | | | | √ | √ | | | | | | | | | | √ | | | | | | |
| 21 | 12.9 | 13.8 | √ | √ | √ | √ | √ | √ | √ | √ | √ | √ | √ | √ | √ | √ | √ | √ | √ | √ | √ | √ | √ | √ | √ | √ | √ |
| 23 | 8.4 | 8.7 | √ | √ | | √ | √ | | | √ | √ | | √ | √ | √ | √ | | √ | | √ | √ | √ | √ | √ | | √ | √ |
| 24 | 9.9 | 8.7 | √ | √ | √ | √ | | | | | | | | | | | | | | | | | | | | | |
| 25 | 10.7 | 6.8 | √ | √ | √ | √ | √ | √ | √ | | | | | | | | | | | | | | | | | √ | √ |
| 26 | 12.1 | 6.4 | √ | | | | √ | | √ | | √ | √ | √ | | | √ | √ | √ | √ | | √ | √ | √ | | √ | √ | |
| 27 | 13.0 | 8.3 | √ | √ | √ | √ | √ | √ | √ | √ | √ | √ | √ | √ | √ | √ | √ | √ | √ | √ | √ | √ | √ | √ | √ | √ | √ |
| 29 | 23.8 | 37.5 | √ | √ | √ | √ | √ | √ | √ | √ | √ | √ | √ | √ | √ | √ | √ | √ | √ | √ | √ | √ | √ | √ | √ | √ | √ |
| 30 | 26.8 | 38.2 | √ | √ | √ | √ | √ | √ | √ | √ | √ | √ | √ | √ | √ | √ | √ | √ | √ | √ | √ | √ | √ | √ | √ | √ | √ |

| | | | | | | | | | | | | | | | | | | | | | | | | | | | |
|--------------|------|------|----|----|----|----|----|----|----|----|----|----|----|----|----|----|----|----|----|----|----|----|----|----|----|----|----|
| 31 | 17.6 | 14.2 | √ | | √ | √ | | √ | √ | | √ | √ | √ | | | | | | | | | | | | | | |
| 65 | 19.9 | 22.8 | √ | √ | √ | √ | √ | √ | √ | √ | √ | √ | √ | √ | √ | √ | √ | √ | √ | √ | √ | √ | √ | √ | √ | √ | |
| 67 | 22.5 | 37.2 | √ | √ | √ | √ | √ | √ | √ | √ | √ | √ | √ | √ | √ | √ | √ | √ | √ | √ | √ | √ | √ | √ | √ | √ | |
| 72 | 22.3 | 43.1 | √ | | | | | | | | √ | | | √ | | √ | √ | | | √ | √ | √ | | | | | |
| 73 | 12.0 | 38.1 | √ | √ | √ | √ | √ | √ | √ | √ | √ | √ | √ | √ | √ | √ | √ | √ | √ | √ | √ | √ | √ | √ | √ | √ | |
| 76 | 10.1 | 23.9 | √ | √ | √ | √ | √ | √ | √ | √ | √ | √ | √ | √ | √ | √ | √ | √ | √ | √ | √ | √ | √ | √ | √ | √ | |
| 77 | 11.2 | 11.2 | | | √ | √ | √ | √ | √ | √ | √ | √ | √ | √ | √ | √ | √ | √ | √ | √ | √ | √ | √ | √ | √ | √ | |
| 78 | 17.5 | 18.2 | | | √ | √ | √ | √ | √ | √ | √ | √ | √ | √ | √ | √ | √ | √ | √ | √ | √ | √ | √ | √ | √ | √ | |
| 63 | 19.8 | 44.0 | | | √ | | | √ | √ | | | | √ | | √ | √ | √ | √ | √ | √ | √ | √ | √ | √ | √ | √ | |
| Total | | | 31 | 25 | 28 | 29 | 27 | 26 | 29 | 26 | 30 | 26 | 26 | 27 | 27 | 28 | 28 | 28 | 26 | 26 | 28 | 28 | 26 | 25 | 23 | 28 | 26 |

546 Note that HP is acronymic of mean height of plant, RL is acronymic of mean root length, species presence is used to designate √,
547 species absence is used to designate blank, and No. is used to designate the species name. The species name list same like
548 supplementary table 1.

549

550

551

552

553

554

555

556

557 **Supplementary Table ST3.** Mean aboveground biomass for September (Biomass of Aboveground), mean plant coverage, and mean
 558 ratio of maximum root depth to the thickness of the active layer (Max root depth: ALT) for groups A (G–A) and B (G–B) over time.

| Year | Biomass of aboveground (g/m ²) | | Plant coverage (%) | | Ratio of max. root depth and ALT | | n | |
|------|--|--------------|--------------------|------------|----------------------------------|-------------|-----|-----|
| | G–A | G–B | G–A | G–B | G–A | G–B | G–A | G–B |
| 1975 | NA | NA | > 60 | > 65 | 0.11 ± 0.09 | 0.14 ± 0.2 | 52 | 27 |
| 1978 | NA | NA | > 60 | > 65 | 0.10 ± 0.07 | 0.14 ± 0.19 | 48 | 20 |
| 1995 | 237.7 ± 8.5 | 250.4 ± 8.5 | 68.2 ± 5.8 | 75.4 ± 5.5 | 0.09 ± 0.05 | 0.15 ± 0.18 | 59 | 22 |
| 1996 | 241.9 ± 9.0 | 249.8 ± 9.7 | 69.8 ± 5.5 | 79.3 ± 7.4 | 0.08 ± 0.03 | 0.16 ± 0.18 | 55 | 23 |
| 1997 | 231.3 ± 9.4 | 251.9 ± 10.2 | 63.3 ± 5.6 | 61.8 ± 6.9 | 0.09 ± 0.01 | 0.18 ± 0.17 | 50 | 25 |
| 1998 | 243.6 ± 9.7 | 247.6 ± 10.4 | 63.8 ± 6.2 | 61.3 ± 4.0 | 0.08 ± 0.01 | 0.15 ± 0.16 | 45 | 29 |
| 1999 | 243.6 ± 9.6 | 245.7 ± 10.0 | 73.3 ± 5.5 | 65.3 ± 6.0 | 0.09 ± 0.02 | 0.15 ± 0.16 | 79 | 31 |
| 2000 | 237.7 ± 8.7 | 246.2 ± 8.5 | 70.8 ± 5.2 | 79.7 ± 7.5 | 0.07 ± 0.02 | 0.15 ± 0.15 | 74 | 31 |
| 2001 | 245.7 ± 8.2 | 248.1 ± 7.9 | 69.1 ± 6.3 | 69.5 ± 8.2 | 0.09 ± 0.03 | 0.15 ± 0.15 | 69 | 29 |
| 2002 | 249.9 ± 7. | 248.9 ± 7.4 | 65.2 ± 6.4 | 67.2 ± 5.6 | 0.09 ± 0.04 | 0.19 ± 0.14 | 64 | 30 |
| 2003 | 232.8 ± 7.8 | 252.7 ± 8.3 | 67.0 ± 5.5 | 57.1 ± 4.9 | 0.10 ± 0.05 | 0.24 ± 0.13 | 60 | 33 |
| 2004 | 241.2 ± 8.7 | 253.4 ± 9.6 | 67.8 ± 6.7 | 59.9 ± 6.9 | 0.08 ± 0.06 | 0.18 ± 0.12 | 78 | 34 |
| 2005 | 238.1 ± 9.1 | 252.7 ± 10 | 56.6 ± 7.4 | 63.1 ± 6.2 | 0.10 ± 0.07 | 0.21 ± 0.12 | 74 | 37 |
| 2006 | 236.0 ± 9. | 253.7 ± 10.1 | 69.3 ± 6.3 | 54.2 ± 5.3 | 0.10 ± 0.08 | 0.18 ± 0.11 | 70 | 39 |
| 2007 | 235.7 ± 9.2 | 254.6 ± 9.7 | 73.8 ± 5.6 | 56.8 ± 6.8 | 0.11 ± 0.04 | 0.19 ± 0.10 | 66 | 20 |
| 2008 | 239.5 ± 9.4 | 254.4 ± 10.1 | 65.7 ± 5.6 | 53.7 ± 7.8 | 0.09 ± 0.02 | 0.21 ± 0.17 | 62 | 24 |
| 2009 | 228.3 ± 9.2 | 252.4 ± 9.6 | 58.7 ± 6.2 | 61.7 ± 8.6 | 0.11 ± 0.00 | 0.21 ± 0.17 | 51 | 28 |
| 2010 | 233.2 ± 8.8 | 249.5 ± 8.9 | 59.6 ± 4.1 | 64.4 ± 8.0 | 0.09 ± 0.03 | 0.16 ± 0.16 | 53 | 30 |
| 2011 | 221.0 ± 8.6 | 244.4 ± 9.1 | 54.4 ± 5.4 | 69.1 ± 6.3 | 0.12 ± 0.05 | 0.16 ± 0.15 | 52 | 33 |
| 2012 | 219.8 ± 8.8 | 233.4 ± 9.3 | 65.6 ± 7.0 | 63.1 ± 7.7 | 0.10 ± 0.04 | 0.17 ± 0.15 | 53 | 33 |
| 2013 | 227.8 ± 8.8 | 247.5 ± 9.3 | 63.2 ± 5.9 | 62.4 ± 9.3 | 0.11 ± 0.03 | 0.18 ± 0.14 | 63 | 34 |
| 2014 | 223.8 ± 9.2 | 229.4 ± 10.0 | 68.0 ± 5.8 | 74.3 ± 10 | 0.11 ± 0.03 | 0.16 ± 0.14 | 69 | 38 |
| 2015 | 229.0 ± 9.4 | 261.5 ± 9.9 | 64.7 ± 6.8 | 66.3 ± 6.6 | 0.12 ± 0.02 | 0.18 ± 0.13 | 57 | 36 |
| 2016 | 237.5 ± 8.6 | 256.5 ± 8.5 | 69.1 ± 5.2 | 67.6 ± 7.6 | 0.13 ± 0.02 | 0.20 ± 0.13 | 52 | 33 |
| 2017 | 233.8 ± 7.1 | 251.5 ± 8.6 | 70.1 ± 6.4 | 65.4 ± 7.1 | 0.12 ± 0.02 | 0.17 ± 0.12 | 50 | 35 |

559 Note: values reported as annual mean \pm SE. Data of the thickness of the active layer (ALT) during 1975-1995 based on the re-analysis
560 from air temperature (ref. 17), during 1996-2017 based on borehole soil temperature (method by ref. 5).

561 **Supplementary Reference**

- 562 1. Ding, L., Zhou, J., Zhang, X., Liu, S., & Cao, R., A long-term 0.01° surface air temperature
563 dataset of Tibetan Plateau. *Data in brief*, 20, 748-752(2018).
564 <https://doi.org/10.1016/j.dib.2018.08.107>
- 565 2. Du Y., Data of climatic factors of annual average temperature in the Xizang (1990–2015).
566 National Tibetan Plateau Data Center, (2019).
567 [https://data.tpdc.ac.cn/en/data/a46b446e-12ac-4ba3-b0b9-
568 1ec6195d2aa8/?q=Data%20of%20climatic%20factors%20of%20annual%20average%20t
569 emperature%20in%20the%20Xizang](https://data.tpdc.ac.cn/en/data/a46b446e-12ac-4ba3-b0b9-1ec6195d2aa8/?q=Data%20of%20climatic%20factors%20of%20annual%20average%20t)
- 570 3. Falge, E., et al., Gap filling strategies for long term energy flux data sets. *Agric. For.*
571 *Meteorol.*, 107(1), 71-77(2001).
572 [https://doi.org/10.1016/S0168-1923\(00\)00235-5](https://doi.org/10.1016/S0168-1923(00)00235-5)
- 573 4. Dengel, S., et al., Testing the applicability of neural networks as a gap-filling method
574 using CH 4 flux data from high latitude wetlands. *Biogeosciences*, 10(12), 8185-8200.
575 (2013).
576 <https://doi.org/10.5194/bg-10-8185-2013>
- 577 5. Wu, Q., & Zhang, T., Changes in active layer thickness over the Qinghai-Tibetan Plateau
578 from 1995 to 2007. *J. Geophys. Res. Atmos.*, 115(D9) (2010).
579 <https://doi.org/10.1029/2009JD012974>
- 580 6. Krinner, G., et al., A dynamic global vegetation model for studies of the coupled
581 atmosphere-biosphere system. *Global Biogeochem. Cycles*, 19(1) (2005).
582 <https://doi.org/10.1029/2003GB002199>
- 583 7. Bjorkman, A. D., et al., Plant functional trait change across a warming tundra biome.
584 *Nat.*, 562(7725), 57-62(2018).
585 <https://doi.org/10.1038/s41586-018-0563-7>
- 586 8. Shaoling, W., Huijun, J., Shuxun, L., & Lin, Z., Permafrost degradation on the Qinghai–
587 Tibet Plateau and its environmental impacts. *Permafr. Periglac. Processes*, 11(1), 43-53
588 (2000).
589 [https://doi.org/10.1002/\(SICI\)1099-1530\(200001/03\)11:1<43::AID-PPP332>3.0.CO;2-H](https://doi.org/10.1002/(SICI)1099-1530(200001/03)11:1<43::AID-PPP332>3.0.CO;2-H)

- 590 9. Yun, H., et al., Consumption of atmospheric methane by the Qinghai–Tibet Plateau
591 alpine steppe ecosystem. *Cryosphere*, 12(9), 2803-2819 (2018).
592 <https://doi.org/10.5194/tc-12-2803-2018>
- 593 10. Wu, X., et al., Environmental controls on soil organic carbon and nitrogen stocks in the
594 high-altitude arid western Qinghai-Tibetan Plateau permafrost region. *J. Geophys. Res.*
595 *Biogeosci.*, 121(1), 176-187(2016).
596 <https://doi.org/10.1002/2015JG003138>
- 597 11. Essington, T. E., Introduction to Quantitative Ecology: Mathematical and Statistical
598 Modelling for Beginners. Oxford University Press (2021).
- 599 12. Kalogirou, S., Destination choice of athenians: An application of geographically weighted
600 versions of standard and zero inflated poisson spatial interaction models. *Geographical*
601 *Analysis*, 48(2), 191-230(2016).
602 <https://doi.org/10.1111/gean.12092>
- 603 13. O'Reilly, M., & Kiyimba, N., Advanced qualitative research: A guide to using theory.
604 London, United Kingdom: Sage (2015).
605 <http://hdl.handle.net/10034/620998>
- 606 14. Queen, J. P., Quinn, G. P., & Keough, M. J., Experimental design and data analysis for
607 biologists. Cambridge university press (2002).
- 608 15. Grace, J. B., Structural equation modeling and natural systems. Cambridge University
609 Press (2006).
- 610 16. Mallet, A. A., A maximum likelihood estimation method for random coefficient
611 regression models. *Biometrika*, 73(3), 645-656(1986).
612 <https://doi.org/10.1093/biomet/73.3.645>
- 613 17. Zou, D., et al., A new map of permafrost distribution on the Tibetan Plateau.
614 *Cryosphere*, 11(6), 2527-2542(2017).
615 <https://doi.org/10.5194/tc-11-2527-2017>
- 616
617
618